

Geochemistry, Geophysics, Geosystems®

RESEARCH ARTICLE

10.1029/2022GC010559

Key Points:

- Basement fault reactivation during Alice Springs Orogeny is pervasive throughout central Australia
- Brittle, shallow crustal deformation dominates central Australia away from the high heat producing central Aileron Province
- Deformation coinciding with the youngest Taramanide orogens is preserved in the Aileron Province due to thermal weakening

Supporting Information:

Supporting Information may be found in the online version of this article.

Correspondence to:

A. L. Nixon,
angus.nixon@adelaide.edu.au

Citation:

Nixon, A. L., Glorie, S., Fernie, N., Hand, M., De Vries Van Leeuwen, A. T., Collins, A. S., et al. (2022). Intracontinental fault reactivation in high heat production areas of central Australia: Insights from apatite fission track thermochronology. *Geochemistry, Geophysics, Geosystems*, 23, e2022GC010559. <https://doi.org/10.1029/2022GC010559>

Received 6 JUN 2022

Accepted 23 OCT 2022

Author Contributions:

Conceptualization: A. L. Nixon, S. Glorie
Formal analysis: A. L. Nixon, N. Fernie
Funding acquisition: S. Glorie
Investigation: A. L. Nixon, N. Fernie
Methodology: D. Hasterok
Resources: G. Fraser
Software: A. T. De Vries Van Leeuwen
Supervision: S. Glorie, A. S. Collins, G. Fraser
Validation: M. Hand, D. Hasterok
Writing – original draft: A. L. Nixon

© 2022. The Authors.

This is an open access article under the terms of the [Creative Commons Attribution License](https://creativecommons.org/licenses/by/4.0/), which permits use, distribution and reproduction in any medium, provided the original work is properly cited.

Intracontinental Fault Reactivation in High Heat Production Areas of Central Australia: Insights From Apatite Fission Track Thermochronology

A. L. Nixon^{1,2}, S. Glorie^{1,2}, N. Fernie³, M. Hand^{1,2}, A. T. De Vries Van Leeuwen^{4,5}, A. S. Collins^{1,2}, D. Hasterok¹, and G. Fraser⁶

¹School of Physical Sciences, Department of Earth and Environmental Science, The University of Adelaide, Adelaide, SA, Australia, ²Mineral Exploration Cooperative Research Centre, The University of Adelaide, Adelaide, SA, Australia, ³Santos, Adelaide, SA, Australia, ⁴UniSA STEM, University of South Australia, Adelaide, SA, Australia, ⁵Mineral Exploration Cooperative Research Centre, University of South Australia, Adelaide, SA, Australia, ⁶Minerals, Energy and Groundwater Division, Geoscience Australia, Canberra, ACT, Australia

Abstract Pervasive intracontinental orogenesis during the Paleozoic has been widely recognized in the metamorphic and structural records of the Aileron Province and Amadeus Basin in central Australia, commonly attributed to the Ordovician–Carboniferous Alice Springs Orogeny. Comparatively less clear, however, is the magnitude and geographic expression of this event elsewhere in the North Australian Craton. This study presents new apatite fission track thermochronology data from central Australia which demonstrate considerable Paleozoic reactivation across the continental interior. Both the Tennant region and Murphy Province exhibit low-temperature cooling coeval with the Alice Springs Orogeny (ca. 450–320 Ma), although Triassic reactivation in the Aileron Province correlates with the timing of the Hunter-Bowen Orogeny (ca. 265–230 Ma) in eastern Australia. High heat production and metasomatism within the Aileron Province has made the region highly susceptible to reactivation, rendering it more vulnerable to subsequent reactivation in response to far-field stresses during the progressive Tasmanides development.

Plain Language Summary It is well known that deformation such as bending and breaking of rocks is focused near boundaries of tectonic plates as they collide with one another. For the last billion years central Australia has been located far from the edges of these plates, yet similar deformation has been found in this region as would be expected close to the plate boundaries. Evidence suggests deformation occurred across much of central Australia at around 400 million years ago, although more local deformation occurred at around 230 million years ago. More recent, localized deformation is only seen in regions which the shallow Earth is unusually hot due to the presence of radioactive elements which make the rocks weaker and easier to break. In both cases, this deformation represents movement and erosion in the upper 3 km of the Earth, likely caused as stresses from the plate boundaries pushed far inland as the Pacific Plate collided with the Australian Plate at this time in eastern Australia. This suggests a much larger geographical impact of this collision, and means we can now predict deformation far inland during this time in addition to the areas close to the plate boundaries where it would be conventionally expected.

1. Introduction

Deformation, metamorphism and structural reactivation in response to evolving forces at the plate boundaries are interpreted to have occurred across much of central and eastern Australia throughout the Paleozoic–Early-Mesozoic. In the North Australian Craton (NAC; Figure 1), the far-field effects of accretionary orogenesis along eastern Gondwana are traditionally grouped together as the Ordovician–Carboniferous Alice Springs Orogeny, but are unevenly distributed across both basement terranes and overlying sedimentary basins (e.g., Nixon et al., 2021; Raimondo et al., 2010, 2014; Spikings et al., 2006). Somewhat counterintuitively, the core of the Alice Springs Orogeny, which exhibits high-grade metamorphism and large-scale crustal shortening, is observed far from any contemporaneous plate margins, in the Aileron and Irindina provinces and along the northern Amadeus Basin in central Australia (Figure 1; Mawby et al., 1999; Raimondo et al., 2011, 2014; Shaw & Black, 1991). Closer to the northern and southern Australian plate margins, only comparatively modest structural reactivation is evident (e.g., Hall et al., 2016; Nixon et al., 2021), with no apparent record of widespread Ordovician–Carboniferous metamorphic disturbance.

Writing – review & editing: S. Glorie,
M. Hand, A. S. Collins, G. Fraser

Disparity in the crustal response to plate-boundary stresses, both in the low- and high-temperature realms, betrays a likely inequality of lithospheric predisposal for strain accommodation across the NAC. Crustal rheology is influenced by a number of factors, including the presence and nature of existing crustal weaknesses, the magnitude of stress transport required for reactivation, the composition of the crust and its thermal lithospheric strength (Raimondo et al., 2010; Ranalli, 2000; Sandiford & Hand, 1998). Of these variables, thermal weakening of the crust is particularly relevant within the NAC, which displays anomalously high heat production from radiogenic elements in Proterozoic rocks (Gard et al., 2019; Hasterok & Gard, 2016; Hasterok & Webb, 2017; McLaren et al., 2003). Although the influence of high heat production on the localization of metamorphism and major deformation in the Aileron Province during the Alice Springs Orogeny is well documented (e.g., Hand & Sandiford, 1999; Raimondo et al., 2010; Sandiford & Hand, 1998), its effect on the low-temperature thermal history of central Australia is yet to be fully explored.

Understanding the expression of deformation within central Australia is a key factor in recognizing the broader nature of intracontinental orogenesis, and advantageous within an exploration context in anticipating the exhumation level of mineralized crust (Glorie et al., 2019). This study aims to further resolve the impact of Paleozoic–Early-Mesozoic

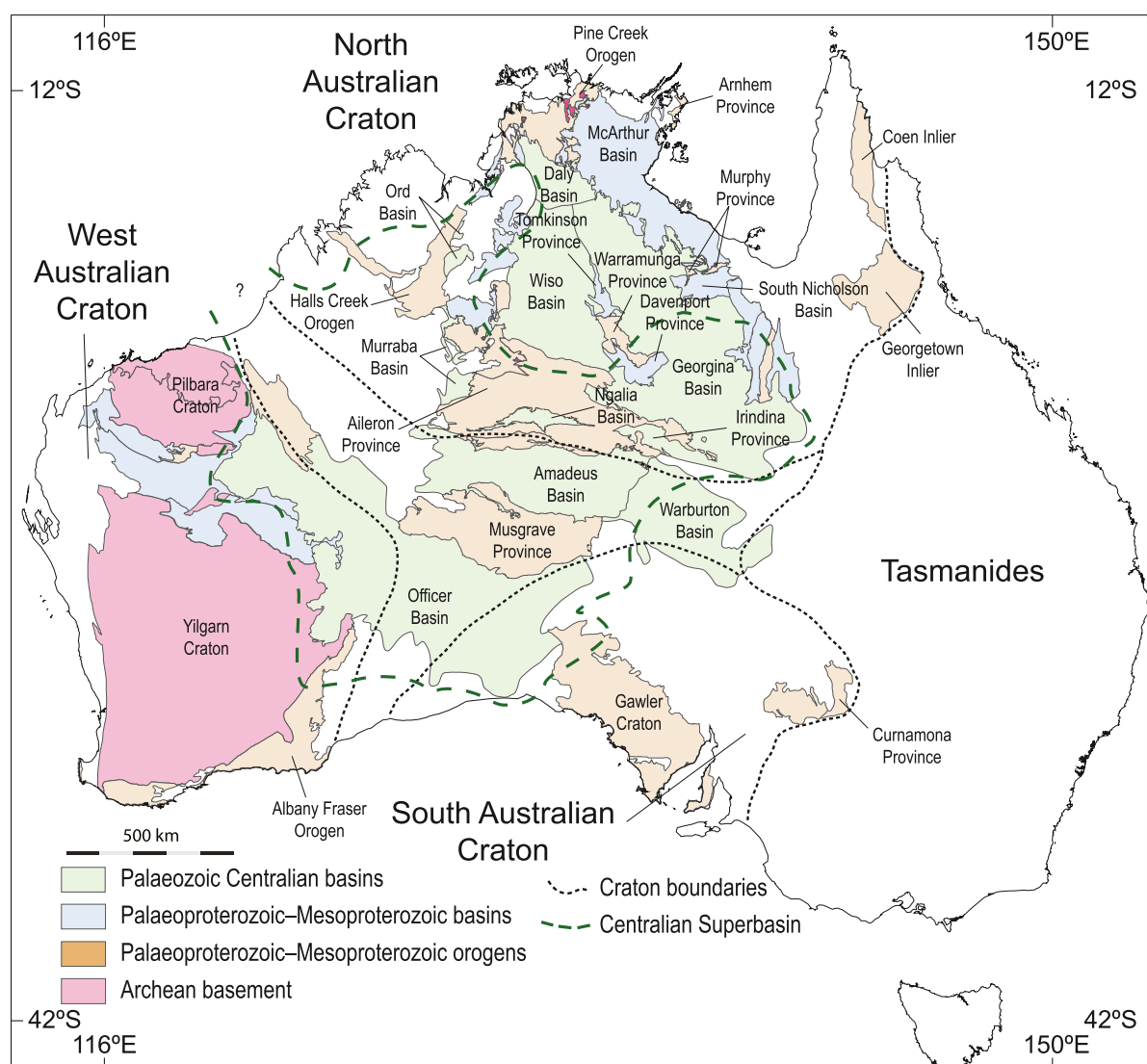


Figure 1. Basic geological regions of Australia, including approximate cratonic divisions of the North Australian Craton, South Australian Craton, West Australian Craton, and Tasmanides (Cawood & Korsch, 2008). Inferred regional extent of the Centralian Superbasin is following Walter et al. (1995) and Ahmad and Munson (2013).

orogenesis on the basement terranes of central Australia, and provides a low-temperature transect from the Aileron Province through the Tennant region and Murphy Province (Figures 1 and 2). New apatite fission track (AFT) data produced from these regions are supplemented by regional topographic and heat production data, in order to rationalize the timing and nature of cooling in a framework of structural and mechanical predisposal to reactivation. This methodology provides a plausible justification of the mechanism for varied cooling observed across the craton, and first-order prediction of terranes most likely to be reactivated during far-field Paleozoic stress regimes.

2. Geological Setting

The NAC comprises an amalgamation of Palaeoproterozoic orogenic basement exposed as inliers between a series of Late-Palaeoproterozoic–Paleozoic basins, with additional thin Cretaceous–Cenozoic cover obscuring relationships between Palaeoproterozoic rocks. The centre of the NAC preserves exposure of the potentially correlative Murphy Province, Tennant region (Warramunga Province, Davenport Province and Tomkinson Province) and Aileron Province (Figures 1 and 2; Claoué-Long, Edgoose, & Worden, 2008; Claoué-Long, Maidment, & Donnellan, 2008; Cross et al., 2020). These basement rocks experienced complex yet discrete deformation and metamorphism events primarily throughout the Palaeoproterozoic, which resulted in considerable Au-Cu-Bi and W mineralization within the Warramunga Province, and lesser mineralization in the Aileron and Murphy provinces (e.g., Ahmad & Wygralak, 1989; Anderson et al., 2013; Compston & McDougall, 1994; Fraser et al., 2008; Howlett et al., 2015; Morrissey et al., 2014; Rawlings et al., 2008; Skirrow et al., 2019). The region was subsequently overlain by Neoproterozoic–Paleozoic sedimentary rocks of the Georgina, Wiso and Ngalia basins, which still cover much of the central NAC (Walter et al., 1995).

2.1. Tennant Region

The Tennant region comprises a number of Palaeoproterozoic basement and sedimentary provinces within the central NAC. The oldest of these is the Warramunga Province, which preserves sedimentary and intrusive rocks aged between ca. 1865–1810 Ma (Claoué-Long, Maidment, & Donnellan, 2008; Maidment, 2013b; Maidment et al., 2013; Page, 1996b, 1996c, 1996d, 1996e). A sequence of siliciclastic and volcanoclastic sedimentary rocks in the *Warramunga Formation*, *Junkali Formation*, and *Woodenjerrie beds* were deposited prior to the ca. 1860–1850 Ma Tennant Creek Event (Compston, 1995; Maidment et al., 2006), and subsequently intruded by dominantly granitic units of the ca. 1850–1840 Ma *Tennant Creek Supersuite* (Figure 2; e.g., Ahmad & Munson, 2013; Maidment et al., 2006, 2013). The Warramunga Province was subsequently overlain by units of the Davenport Province, primarily in the southern Warramunga Province, with more limited cover in the north and west. The Davenport Province units consist of a mixture of volcanic and siliciclastic sequences deposited between ca. 1850–1810 Ma, separated into the *Ooradidgee Group* and *Hatches Creek Group* (Claoué-Long, Maidment, & Donnellan, 2008; Compston, 1995; Maidment et al., 2006, 2013). Additional igneous units of the intrusive and extrusive *Treasure Suite* (ca. 1820–1810 Ma; Claoué-Long, Maidment, & Donnellan, 2008; Maidment et al., 2006) and intrusive *Devils Suite Group* (ca. 1720–1710 Ma; Donnellan & Johnstone, 2004; Maidment et al., 2006) are preserved within the Warramunga and Davenport provinces, and constitute the youngest magmatic rocks observed in the region.

The northern Tennant region is overlain by sedimentary rocks of the Tomkinson Province, which overlie successions of the *Ooradidgee Group* (e.g., Ahmad & Munson, 2013; Donnellan et al., 1995). Tomkinson Province units are preserved as dominantly siliciclastic sequences of sandstone to siltstone with subordinate carbonaceous units, divided into the *Tomkinson Creek Group*, *Namerinni Group*, and *Renner Group* which are separated by regional unconformities (Donnellan et al., 1995, 2001; Hussey et al., 2001). Sedimentary rocks of the Tomkinson Province are likely correlatives of successions in the McArthur Basin to the north of the Tennant region (Donnellan et al., 2001; Hussey et al., 2001; Yang et al., 2020), placing deposition of Tomkinson strata at ca. 1810–1325 Ma (Ahmad & Munson, 2013; Nixon, Glorie, Collins, et al., 2022).

2.2. Murphy Province

The Murphy Province comprises Palaeoproterozoic metasedimentary and felsic intrusive to volcanic rocks, outcropping in the northeastern NAC (Figures 1 and 2). Turbiditic greywacke and shale metamorphosed to

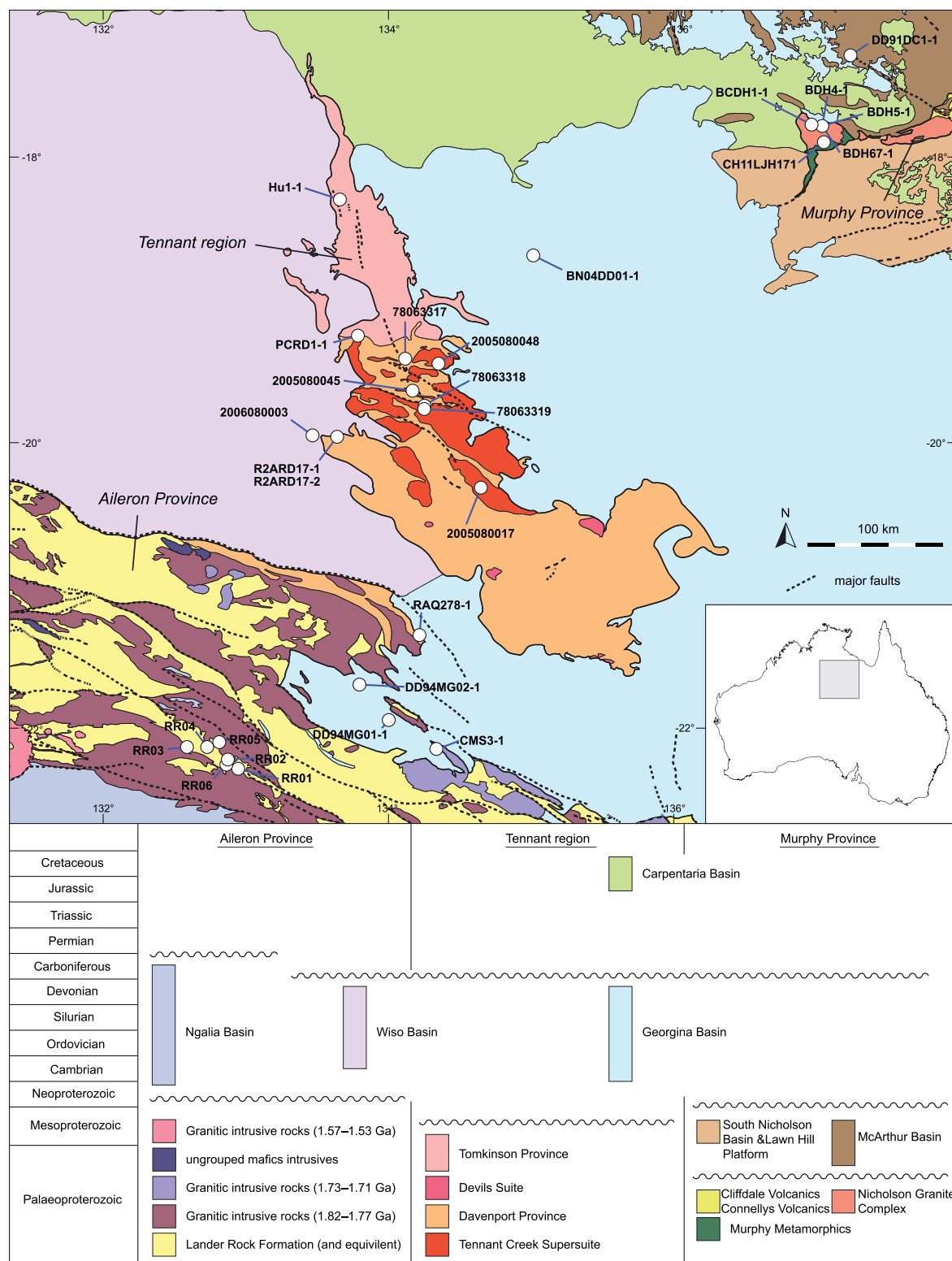


Figure 2. Major geology of the central Northern Territory. Due to the complexity of intrusive units within the Aileron Province, granitic units have been grouped by age. Locations of all samples analyzed in this study are shown by circles. Inset shows location of study area within Australia.

greenschist facies of the *Murphy Metamorphics* (Ahmad & Wygralak, 1989; Rawlings et al., 2008) represent the oldest recognized units within the Murphy Province, with protolith deposition constrained between 1853 ± 4 and 1845 ± 3 Ma (Hollis et al., 2010; Page et al., 2000). Metamorphism to greenschist facies is interpreted as prior to regional intrusion by the *Nicholson Granite Complex* and extrusion of volcanic units. Felsic extrusive units of the *Cliffdale Volcanics* and *Connellys Volcanics* appear as a comagmatic suite with the *Nicholson Granite Complex* at ca. 1855–1845 Ma (Page et al., 2000), and unconformably overlie the *Murphy Metamorphics*. Exposure of the Murphy Province is limited, as basement is unconformably overlain by sedimentary basins of the Palaeoproterozoic–Mesoproterozoic McArthur Basin and South Nicholson Basin (Figure 1), and the Cryogenian–Devonian Georgina Basin (Ahmad & Wygralak, 1989; Rawlings et al., 2008). The Georgina Basin extends westward from the Murphy Province and overlies the eastern extent of the Warramunga, Davenport and Tomkinson provinces (Donnellan et al., 2001; Walter et al., 1995).

2.3. Aileron Province

The Aileron Province is situated in the southern NAC, and comprises Palaeoproterozoic igneous and metasedimentary units (Figures 1 and 2). The oldest observed units in the Aileron Province are metasediments of the *Lander Rock Formation* (and correlatives) and Casey Inlier deposited at ca. 1860–1830 Ma (Carson et al., 2011; Donnellan, 2008; Worden et al., 2008). Pelitic and psammitic units of the *Lander Rock Formation* exhibit variable, complex metamorphism from greenschist to granulite facies (e.g., Claoué-Long, Edgoose, & Worden, 2008; Young et al., 1995), and are believed to correlate with the *Ooradidgee Group* of the Davenport Province (Claoué-Long et al., 2008a, 2008b). Extensive magmatism, metamorphism and deformation occurred within the Aileron Province periodically between ca. 1820–1130 Ma (e.g., Ahmad & Munson, 2013; Close et al., 2007; Hoatson et al., 2005; Worden et al., 2008).

2.4. Neoproterozoic–Paleozoic Basins

Following the late-Palaeoproterozoic, a period of prolonged sedimentation prevailed within the NAC, resulting in the formation of the widespread greater McArthur Basin system overlying the orogenic basement (Close, 2014). Extensive contiguous successions were subsequently deposited across the West Australian Craton (WAC) and NAC in the interconnected Centralian Superbasin (Figure 1), with deposition in central Australia during the Neoproterozoic observed in the Amadeus, Georgina, Murraba, Officer and Ngalia basins (Ahmad & Munson, 2013; Walter et al., 1995). Sedimentation in these basins continued up to the ca. 580–530 Ma Petermann Orogeny (Raimondo et al., 2010), after which the basin system migrated away from the WAC and was almost exclusively confined within the NAC. This younger depositional phase saw coeval sedimentation of syn-tectonic detritus within the Amadeus, Georgina, Ngalia, Wiso Ord, Daly and Warburton basins in the Cambrian–Ordovician (Ahmad & Munson, 2013; Walter et al., 1995). Paleozoic deposition within the superbasin was disrupted by the ca. 450–320 Ma Alice Springs Orogeny, although significant sourcing of detritus to evolving basins is also attributed to this event (Haines et al., 2001).

2.5. Paleozoic Deformation

2.5.1. Central Australia

Multiple intracontinental deformational events have been observed in central Australia within the metamorphic and sedimentary records in the Paleozoic, subsequent to cratonic amalgamation and primary orogenesis. The Late-Neoproterozoic–Early-Cambrian Petermann Orogeny (ca. 580–530 Ma) exhumed large sections of the Musgrave Province during extensive thrusting along east–west striking faults, and is associated with regional high-grade metamorphism of basement granites and gneisses (Hand & Sandiford, 1999; Raimondo et al., 2010; Walter et al., 1995). Similar style deformation during the Late-Ordovician–Carboniferous Alice Springs Orogeny (ca. 450–320 Ma) was focused further north in the Aileron and Irindina provinces and northern Amadeus Basin (e.g., Haines et al., 2001; Shaw & Black, 1991; Shaw et al., 1979). Both orogenic events are characterized by crustal-scale north-south shortening and high-grade metamorphism in the Musgrave (Petermann Orogeny), Aileron and Irindina provinces and the Amadeus Basin (Alice Springs Orogeny), and metamorphic reworking appears confined within these provinces. Preservation of extensive syn-orogenic detritus in contemporary basins

across northern Australia and structural reactivation in distal Palaeoproterozoic basement, however, suggests the deformational extent of these events reached far wider across the NAC (e.g., Glorie, Agostino, et al., 2017; Haines et al., 2001; Nixon et al., 2021).

2.5.2. Tasmanides

Contemporaneous with and post-dating the central Australian Alice Springs Orogeny, progressive accretion and deformation of the Tasmanides occurred at the eastern Australian margin from ca. 515–230 Ma (e.g., Coney et al., 1990; Glen et al., 2009; Rosenbaum, 2018; Rosenbaum et al., 2012). The Tasmanides encompass a number of orogenic events, beginning with the ca. 515–490 Ma Delamerian Orogeny (e.g., Boger & Miller, 2004; Foden et al., 2006; Jenkins & Sandiford, 1992; Withnall et al., 1996) and continuing to the ca. 265–230 Ma Hunter-Bowen Orogeny (Babaahmadi et al., 2017; Jessop et al., 2019; Rosenbaum et al., 2012), typified by west-directed oceanic subduction below the continental Australian plate. Orogenesis at the eastern margin terminated with sustained trench retreat following the Hunter-Bowen Orogeny at ca. 230 Ma, which marks the youngest regional-scale deformation in eastern Australia (e.g., Coney et al., 1990; Jessop et al., 2019; Li et al., 2012).

3. Materials and Methods

3.1. Sampling Strategy

Samples were obtained from the Tennant region, Murphy Province and Aileron Province from a combination of field samples and shallow drill core targeting igneous and tuffaceous units, to create a transect from the Aileron Province to the Murphy Province (Figure 2). A total of nine samples were obtained from drill core around the Tennant region, supplemented by an additional three surface samples. A further 10 samples were collected from the Aileron Province, with four samples collected from the northern Aileron Province near onlap of the Georgina Basin, and six samples from the Anmatjira Range in the central Aileron Province. From the Murphy Province, five samples were obtained from drill core and one from a surface field sample. Full sample locations and depth ranges are provided in Table 1. The majority of samples were collected from open file drill core during the course of this study, while samples 2006080003, 78063317, 78063318, and 78063319 were sourced from drill core provided by Geoscience Australia, and samples CH11LJH171, 2005080017, 2005080045, and 2005080048 were sourced from field samples provided by Geoscience Australia and the Northern Territory Geological Survey. Previous U–Pb geochronology for these samples is provided in Black (1984), Kositcin et al. (2013), and Maidment et al. (2013).

3.2. Processing

Apatite grains were separated at the University of Adelaide using conventional crushing procedures, followed by panning, Frantz magnetic separation, and immersion in liquid lithium heteropolytungstate, diluted to specific gravity of 2.85 gcm^{−3}. Grains were mounted in EpoxyCure2 resin, ground with #2000 silicon carbide paper to expose grain cores and polished with 3 and 1 μm diamond paste (e.g., Glorie, Alexandrov, et al., 2017), and mounts were subsequently etched with 5 M HNO₃ at 20 ± 0.5°C for 20 ± 0.5 s to reveal spontaneous fission tracks.

3.3. Apatite Fission Track Thermochronology

Apatite grains were imaged with a Zeiss AXIO Imager M2m Autoscan microscope system at the University of Adelaide prior to microprobe and laser analysis. Mounts were coated with a ~5 nm thick gold coating prior to imaging to minimize internal reflections. Fission track densities and confined track lengths were manually identified using FastTracks software. Following laser ablation, the samples were reground by ~10 to 8 μm prior to polishing and irradiated with a ²⁵²Cf source to reveal additional confined tracks for use in modeling (Donelick & Miller, 1991).

Table 1

Sample Lithology and Locations for All Apatite Fission Track Samples, With Coordinates Provided in GDA94 System

Sample	Well	Unit	Lithology	Latitude	Longitude	Elevation (m)	Depth (m)	Inclination
<i>Aileron Province</i>								
CMS3-1	CMS3	Granite (unassigned)	Granite	−22.1429	134.3393	539	155.8–158.8	3°
DD94MG01-1	DD94MG01	Granite (unassigned)	Granite	−21.9431	134.0023	528	412.5–414.0	–
DD94MG02-1	DD94MG02	Granite (unassigned)	Granite	−21.6961	133.7966	509	168.5–170.6	–
RAQ278-1	RAQ278/DD1	Granulite (unassigned)	Granulite	−21.3485	134.2182	456	9.9–12.3	45°
RR01	Field sample	Anmatjira Granite	Granite	−22.1307	132.5887	711	0	–
RR02	Field sample	Anmatjira Orthogneiss	Gneissic granite	−22.1371	132.7297	692	0	–
RR03	Field sample	Anmatjira Orthogneiss	Gneissic granite	−22.0978	132.8143	654	0	–
RR04	Field sample	Anmatjira Orthogneiss	Gneissic granite	−22.2171	132.8753	645	0	–
RR05	Field sample	Harverdon Granite	Granite	−22.2548	132.8673	659	0	–
RR06	Field sample	Mount Airy Orthogneiss	Gneissic granite	−22.2827	132.9435	685	0	–
<i>Tennant Region</i>								
2005080017	Field sample	Hill of Leaders Granite	Granite	−20.3142	134.6488	418	0	–
2005080045	Field sample	Airport Porphyry	Felsic porphyry	−19.6390	134.1701	366	0	–
2005080048	Field sample	Tennant Creek Granite	Granite	−19.4457	134.3510	334	0	–
2006080003	RV12ARD2	Rover Field Volcaniclastic	Felsic volcaniclastic	−19.9514	133.4685	299	456.9–458.2	18°
78063317	DDH 11 BMR-NTGS	Bernborough Formation	Rhyolite	−19.4123	134.1179	333	39.9–46.1	–
78063318	DDH 1 BMR-NTGS	Tennant Creek Granite	Granite	−19.7457	134.2510	342	103.0–113.0	–
78063319	Unnamed drill site	Cabbage Gum Granite	Gneissic granite	−19.7582	134.2537	346	153.3–160.9	–
BN04DD01-1	BN04DD01	Helen Springs Volcanics	Intermediate volcanics	−18.6888	135.0158	208	440.5–443.1	–
Hu1-1	Hunter 1DD	Barney Creek Formation	Tuff	−18.2968	133.6604	264	414.5–414.6	–
PCRD1-1	PCRD001	Warrego Granite	Granite	−19.2489	133.7824	338	152.8–155.2	30°
R2ARD17-1	R2ARD17	Warramunga Formation	Dacite	−19.9586	133.6407	292	108.9–111.4	30°
R2ARD17-2	R2ARD17	Warramunga Formation	Dacite	−19.9586	133.6407	292	365.5–368.4	30°
<i>Murphy Province</i>								
BCDH1-1	BCDH1	Nicholson Granite Complex	Granite	−17.7720	136.9650	273	42.0–60.0	–
BDH4-1	BDH4	Nicholson Granite Complex	Granite	−17.7809	137.0406	250	86.5–89.1	30°
BDH5-1	BDH5	Nicholson Granite Complex	Granite	−17.7814	137.0408	251	53.0–55.3	30°
BDH67-1	BDH67	Nicholson Granite Complex	Granite	−17.7819	137.0404	251	46.6–49.9	30°
CH11LJH171	Field sample	Nicholson Granite Complex	Granite	−17.8942	137.0541	260	0	–
DD91DC1-1	DD91DC1	McDermott Formation	Tuff	−17.2858	137.2384	248	186.6–186.7	–

Note. Elevation is the surface point elevation of the sampled location following the Global Multi-resolution Terrain Elevation Data topographic imagery (Danielson & Gesch, 2011). Depth is the measured drilled depth from which samples were taken below surface elevation, and Inclination is the approximate deviation from vertical for the drill hole, where applicable.

3.4. Electron Probe Micro Analysis

Apatite major and minor elemental concentrations were determined by electron probe micro analysis (EPMA) at Adelaide Microscopy using a Cameca SXFive Electron Microprobe fitted with LTAP, PCO, LLIF and two LPET crystals. Samples were polished with 1 μm diamond paste to remove any residual gold coating, then carbon coated to remove excess charging during EPMA. Analysis was conducted in a single stage analytical protocol with a 5 μm beam diameter at an accelerating voltage of 10 kV and beam current of 15 nA, as outlined by Nixon et al. (2021). Samples were analyzed across three analytical sessions (sessions EPMA-19, EPMA-21, and EPMA-22), and Durango apatite was interspaced within analytical sequences and served as a secondary standard.

3.5. LA-ICP-MS Analysis

Isotopic data were acquired by LA-ICP-MS using a RESolution LR 193 nm excimer laser connected to an Agilent 7900× ICP-MS at Adelaide Microscopy. Durango apatite was interspaced as a secondary standard throughout analytical sessions to serve as an accuracy check. Data collection was performed in four analytical sessions (sessions LA-18, LA-19a, LA-19b, and LA-21). Geochemical data were reduced using the “X_Trace_Elements_IS” data reduction package of Iolite v3.32 software (Paton et al., 2011), using NIST610 as the primary standard.

3.6. Fission Track Age Calculation

Fission track ages were calculated using the LA-ICP-MS method, using ^{238}U concentrations and fission track densities to calculate single grain ages. Single grain and population ages were calculated using IsoplotR software (Vermeesch, 2018) using a session-specific zeta calibration calculated from parallel analysis of a Durango apatite standard (Vermeesch, 2017).

3.7. Thermal History Modeling

Thermal history modeling was undertaken with QTQt software (Gallagher, 2012), using inputs of AFT single grains ages, confined track length distributions, and using r_{mr0} as the kinetic parameter (Carlson et al., 1999). The r_{mr0} multi-kinetic parameter is advantageous over other single-kinetic parameters as it considers total grain chemistry and is therefore less vulnerable to decoupling between single-kinetic variables and absolute grain retentivity (McDannell et al., 2019; Powell et al., 2018). The r_{mr0} value was calculated for each grain using EPMA-derived halogen compositions and LA-ICP-MS obtained trace element concentrations, following Ketcham et al. (1999) and Nixon et al. (2021). Mapped and sub-surface geology was also considered and included as model constraints where applicable, in order to further refine the reconstructions (e.g., Green & Duddy, 2021), using an assumed geothermal gradient of $\sim 30^\circ\text{C}/\text{km}$ to calculate vertical temperature variations (Holgate & Gerner, 2010). The R2ARD17 drill hole to the west of outcropping basement in the Tennant region cuts through sediments of the Wiso Basin before intersecting weathered volcanics of the underlying Warramunga Province (Adelaide Resources Ltd., 2010). The unconformity between the Wiso Basin and Warramunga Province was used as a constraint for sample depth below this surface immediately prior to deposition of lower Wiso Basin sediments at ca. 520–510 Ma (Kennewell & Huleatt, 1980; Kruse, 1998; Traves, 1955). Similarly, igneous basement of the Aileron Province is unconformably overlain by the *Central Mount Stuart Formation* of the Georgina Basin in the CMS3 and DD94MG01 drill holes (Chuck, 1982; Menzies & Louwrens, 1995), allowing for inference of a constraint placing this interface at the surface immediately prior to deposition of this unit at ca. 580–530 Ma (Ahmad & Munson, 2013; Dunster et al., 2007; Walter et al., 1989). The RAQ278/DD1 drill hole in the northern Aileron Province does not preserve overlying Georgina Basin sedimentary rocks (Northern Territory Geological Survey, 1983), however, based on the nearby presence of outcropping *Central Mount Stuart Formation* (Haines, 1991), a similar constraint has been added for this drill hole to be consistent with other drill holes in this region. Unconformities were not recognized in the vicinity of samples 2005080017, CH11LJH171, RR01, RR04, and RR06, nor observed in drill holes PCRD001, Hunter 1DD, DDH 11 BMR-NTGS, RAQ278/DD1, DD94MG01, CMS3, BCDH1, BDH4, BDH5, BDH67, and DD91DC1, hence these samples have been modeled without post-depositional constraints. Full modeling rationale and residuals are provided in Supporting Information S1.

4. Results

4.1. Geochemistry

4.1.1. Data Accuracy

Durango apatite returned weighted mean halogen concentrations of 3.37 ± 0.01 wt% F and 0.43 ± 0.01 wt% Cl for the secondary standard analyzed in session EPMA-19, weighted mean halogen concentrations of 3.55 ± 0.01 wt% F and 0.37 ± 0.01 wt% Cl in session EPMA-21, and weighted mean halogen concentrations of 3.49 ± 0.01 wt% F and 0.37 ± 0.01 wt% Cl in session EPMA-22. Different crystals were analyzed in each analytical session, but no obvious drift was observed within sessions. The measured Durango apatite chemistry across analytical

sessions is consistent with published concentrations (3.35 ± 0.13 wt% F; Marks et al., 2012; ~ 0.46 to 0.37 wt% Cl; Chew et al., 2016), suggesting compositional EPMA data is reliable. Halogen weighted mean plots for Durango secondary standards are provided in Supporting Information S1.

4.1.2. Geochemistry Results

All analyzed apatites in this study can be regarded as fluorapatites, and retain uniform intra-sample geochemistry with little variation in retentivity between samples. The majority of apatites yield relatively low retentivity values, where apatites from the Tennant region preserve average r_{mr0} values of 0.91–0.84 and apatites from the Aileron Province preserve average r_{mr0} values of 0.89–0.87. The majority of samples from the Murphy Province preserve average r_{mr0} values of 0.84–0.83, while a single tuff sample (DD91DC1-1) preserves a more retentive average r_{mr0} of 0.74. Common fluorapatites typically yield r_{mr0} values of 0.83–0.81, which suggests most samples examined in this study are less retentive than average apatites.

4.2. Apatite Fission Track Data

4.2.1. Data Accuracy

Single-grain AFT ages were calibrated using a session-specific zeta factor based on Durango apatite AFT data, following Vermeesch (2017). Analyzed Durango apatite returned weighted mean AFT ages of 28.3 ± 3.1 (Session LA-18), 28.7 ± 2.9 (Session LA-19a), 28.8 ± 2.6 (Session LA-19b), and 31.7 ± 2.0 Ma (Session LA-21), all of which are within uncertainty of the published standard $^{40}\text{Ar}/^{39}\text{Ar}$ age (31.44 ± 0.18 Ma; McDowell et al., 2005), suggesting that fission track analysis was reliable and AFT ages can be used with confidence.

4.2.2. Apatite Fission Track Results

Radial plots for all samples of this study exhibit low single-grain age-dispersion, without open-jaw characteristics (O'Sullivan & Parrish, 1995) or age variation coupled with retentivity variation (individual radial plots and r_{mr0} comparisons are provided in Supporting Information S1). Single-grain age dispersion is consistently low ($<20\%$) with the exception of samples RR02 and RR05, hence nearly all samples are interpreted as preserving only single, central age populations (Table 2). The radial plots for higher dispersion samples RR02 and RR05 (37%–33%) do not display significant open-jaw characteristics (O'Sullivan & Parrish, 1995), so only central ages have been quoted, although it is possible these samples experienced more complex thermal histories (Supporting Information S1). Chi-square values vary considerably across samples, and the chi-square test is failed ($P(\chi^2) < 0.05$) by populations within samples CMS3-1, DD94MD01-1, 78063317, 78063318, PCRD1-1, BDH4-1, BDH5-1, and samples RR01–RR06 (Table 2). It should be noted, however, that old, high-U samples such as those in central Australia can return inappropriately low chi-square values due to the high precision achieved using the LA-ICP-MS method (McDannell, 2020), hence dispersion and open/closed-jaw trends are considered more appropriate for interpretation of multiple discrete age populations. Samples from the central Aileron Province (RR01–RR06) yield some of the youngest AFT central ages from this study between 265 and 183 Ma, comparable to sample CMS3-1 from the northern Aileron Province which preserves an age of 197 ± 7 Ma. In contrast, samples DD94MD01-1, DD94MD02-1 and RAQ278-1 from the northernmost region of the Aileron Province skew slightly older between 322 and 225 Ma. AFT ages from the Tennant region again skew older than those observed within the Aileron Province, preserving a wide range of AFT central ages between ca. 409–236 Ma (Figure 3). The Murphy Province yielded the least variation within central ages, preserving AFT ages between ca. 384–323 Ma. A total of 18 samples yielded sufficient confined fission tracks for interpretation (≥ 50), with samples spread across the Aileron, Tennant and Murphy regions (Table 2). Confined track distributions are all unimodal, preserving weakly to moderately negatively skewed distributions (Supporting Information S1). All samples retain mean track lengths ranging between 12.7 ± 1.5 to 11.4 ± 1.3 μm , generally suggesting significant residence within the apatite partial annealing zone (APAZ; $\sim 120^\circ\text{C}$ to 60°C ; Gleadow et al., 1986; Wagner & Van den haute, 1992).

The thermal history model for the R2ARD17 drill hole on the western flank of the Warramunga Province of the Tennant region exhibits a gradual heating, entering the shallow APAZ at ca. 500 Ma (Figure 4), followed by slow monotonic cooling with no evidence for subsequent thermal perturbations until present day. In the northern Aileron Province, the modeling results for samples RAQ278/DD1 and DD94MG01 similarly predict heating to shallow APAZ temperatures of $\sim 80^\circ\text{C}$ at ca. 450–350 Ma, followed by slow cooling to present day temperatures

Table 2
Summary of Apatite Fission Track (AFT) Results

Sample ID	$\rho_s (\times 10^6/\text{cm}^2)$	N_s	n	$U \pm 2\sigma$ (ppm)	C. age (Ma)	$P(\chi^2)$	Disp. (%)	n_i	MTL ± 1 SD (μm)	r_{mr0}
<i>Aileron Province</i>										
CMS3-1	2.0170	1,624	35	18.5 ± 0.6	197 ± 7	0.01	12	102	12.5 ± 1.4	0.87–0.88
DD94MD01-1	1.6107	1,109	34	10.8 ± 0.3	265 ± 10	0.03	12	128	12.2 ± 1.4	0.86–0.87
DD94MD02-1	2.5441	614	26	20.8 ± 1.1	225 ± 11	0.22	9	–	–	0.87–0.92
RAQ278-1	0.9305	479	38	6.6 ± 0.2	322 ± 15	0.79	0	81	12.4 ± 1.7	0.87–0.88
RR01	3.5322	3,860	39	40.7 ± 0.7	186 ± 4	0.00	10	168	12.7 ± 1.2	0.86–0.88
RR02	0.8050	853	31	8.1 ± 0.4	254 ± 18	0.00	33	–	–	0.87
RR03	0.6958	411	17	6.9 ± 0.3	210 ± 15	0.03	18	–	–	0.89
RR04	2.5560	2711	30	29.1 ± 1.0	183 ± 8	0.00	22	84	12.7 ± 1.5	0.87
RR05	0.5509	686	37	4.7 ± 0.2	256 ± 18	0.00	37	–	–	0.87
RR06	1.9112	1,572	32	22.3 ± 1.0	187 ± 8	0.00	19	84	12.5 ± 1.4	0.87–0.88
<i>Tennant Region</i>										
2005080017	5.459	1,099	20	47.1 ± 2.0	240 ± 9	0.19	5	112	12.1 ± 1.6	0.87
2005080045	2.5876	93	3	13.8 ± 0.5	354 ± 40	0.42	0	–	–	0.87–0.88
2005080048	1.5787	369	22	8.3 ± 0.7	375 ± 22	0.27	7	–	–	0.87
2006080003	1.2263	584	28	6.8 ± 0.3	369 ± 19	0.08	14	–	–	0.86–0.87
78063317	1.5461	823	38	8.0 ± 0.3	352 ± 15	0.01	16	121	12.1 ± 1.5	0.87–0.88
78063318	9.0962	3,288	30	56.0 ± 1.3	290 ± 7	0.00	9	–	–	0.89–0.93
78063319	1.0499	756	35	6.4 ± 0.2	301 ± 13	0.06	12	–	–	0.86–0.87
BN04DD01-1	2.3596	261	9	14.9 ± 0.6	277 ± 17	0.23	0	–	–	0.86–0.87
Hu1-1	1.0714	647	35	5.7 ± 0.2	342 ± 14	0.69	0	134	12.3 ± 1.4	0.83–0.85
PCRD1-1	4.3367	1,889	27	32.9 ± 1.1	236 ± 7	0.01	10	173	12.5 ± 1.2	0.86–0.87
R2ARD17-1	1.7035	660	36	7.6 ± 0.3	409 ± 17	0.14	7	100	12.3 ± 1.5	0.85–0.87
R2ARD17-2	1.3005	401	31	7.1 ± 0.2	339 ± 17	0.94	0	88	12.1 ± 1.5	0.85–0.87
<i>Murphy Province</i>										
BCDH1-1	2.4031	583	26	15.3 ± 0.6	324 ± 16	0.19	12	154	12.3 ± 1.3	0.82–0.86
BDH4-1	4.1373	832	26	24.2 ± 0.8	343 ± 17	0.01	16	63	11.7 ± 1.5	0.81–0.85
BDH5-1	3.8426	650	21	21.4 ± 0.8	356 ± 19	0.02	14	122	11.9 ± 1.4	0.81–0.85
BDH67-1	2.7978	670	30	17.3 ± 0.6	323 ± 13	0.59	6	100	12.4 ± 1.5	0.81–0.84
CH11LJH171	4.5511	472	8	23.3 ± 0.5	384 ± 20	0.51	0	50	11.4 ± 1.3	0.82–0.86
DD91DC1-1	1.6574	808	31	8.9 ± 0.3	380 ± 14	0.89	0	193	12.3 ± 1.5	0.65–0.80

Note. ρ_s represents the average surface density of spontaneous fission tracks. N_s is the total number of spontaneous fission tracks counted in the sample. n is the number of grains analyzed in the sample. U is the average concentration of uranium for all grains in the sample, with uncertainty given as 2σ . C. age is the sample AFT central age as calculated using IsoplotR software (Vermeech, 2018), where all errors represent 1σ . $P(\chi^2)$ is the chi-square probability that all grains in the population may be attributed to a single age population. Disp. is the percentage of dispersion within the sample AFT ages. n_i is the number of confined tracks measured for all grains of the sample. MTL is the mean confined track length, with uncertainty quoted as one standard deviation. r_{mr0} is the range of r_{mr0} values measured within each sample.

(Figure 4). In the central Aileron Province sample RR01, RR04, and RR06 preserve notably different cooling profiles, displaying rapid cooling at ca. 230–200 Ma, while cooling of this age is further observed in the CMS3 well in the northern Aileron Province (Figure 4). Samples from the central Tennant region exhibit varied cooling profiles (Figure 4). The DDH 11 BMR-NTGS (sample 78063317) and Hunter 1DD drill holes predict fast cooling events at ca. 450–400 Ma, while fast cooling in the PCRD001 drill hole is modeled at ca. 290 Ma. Modeled cooling for the field sample 2005080017 is slower, beginning at ca. 400 Ma and cooling below the APAZ until

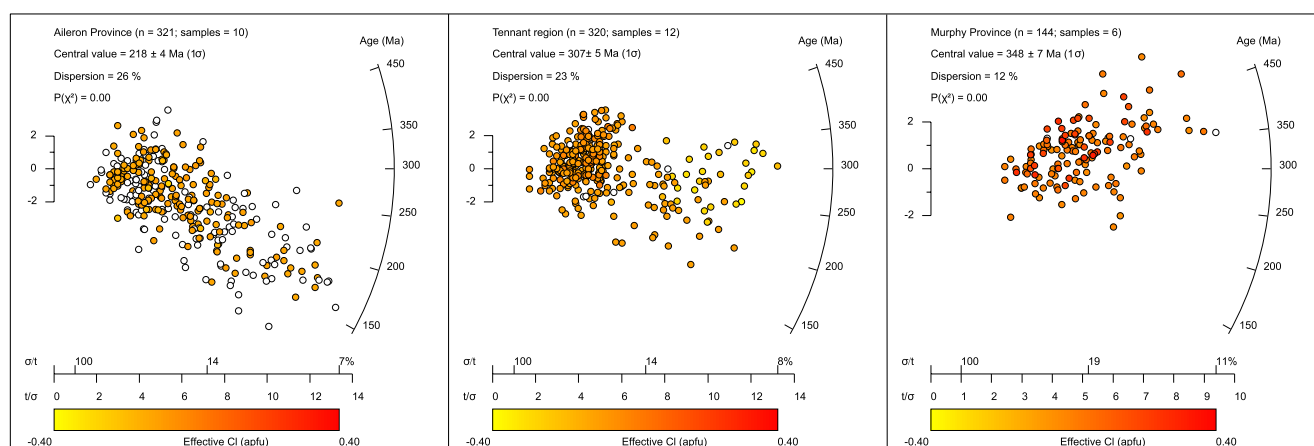


Figure 3. Pooled apatite fission track radial plots for samples from the Aileron Province, Tennant region and Murphy Province. Single-grain ages are colored by effective Cl content derived from grain r_{mro} values as outlined in Ketcham et al. (1999) and Nixon et al. (2021), for easier comparison with the more conventional Cl kinetic parameter.

ca. 240 Ma. The thermal history models from the Murphy Province are more uniform and predict slow monotonic cooling trends from ca. 450–300 Ma in this region, facilitating cooling of at least 40°C during this period (Figure 4).

5. Discussion

5.1. Silurian–Carboniferous

The low-temperature thermal history of central Australia is dominated by widespread cooling in the Silurian–Carboniferous, coinciding with intracratonic deformation during the Alice Springs Orogeny. This is particularly evident within the Tennant region, which records notable fast cooling during this time (Figure 4). In the heavily faulted Warramunga Province, which crops out in the central Tennant region in the central NAC, the thermal history models record fast cooling of >40°C, at ca. 450–400 Ma and ca. 300–270 Ma (Figures 4–6). The ca.

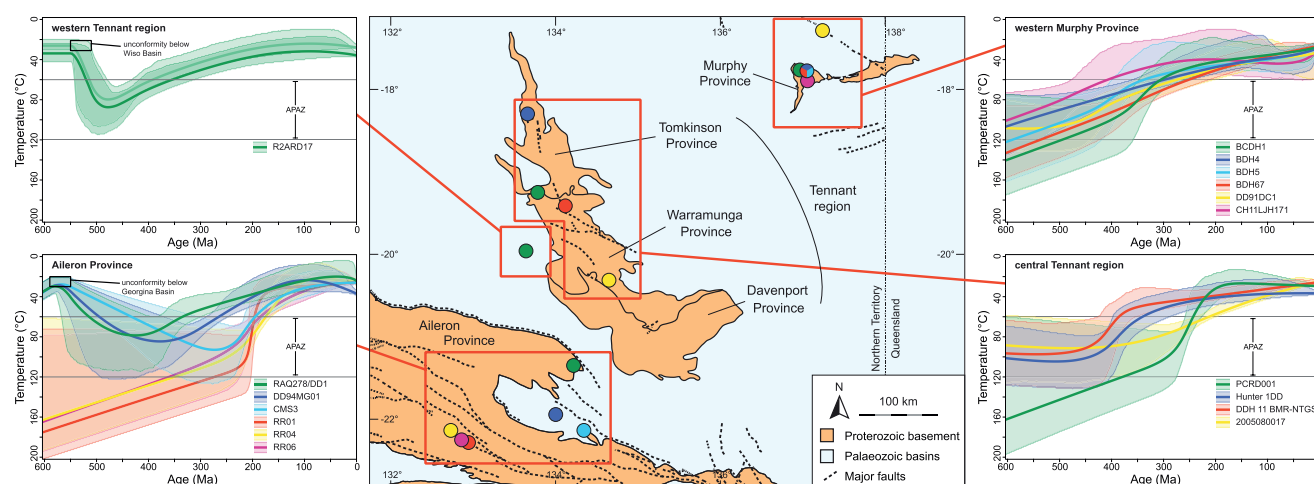


Figure 4. Low-temperature thermal history models for samples from the western Tennant region, central Tennant region, Aileron Province and western Murphy Province, produced using QTQt software (Gallagher, 2012). Sample 2005080017 is a field sample taken at surface, while all other models are presented by sampled well. Solid lines denote the “expected” thermal history, while faded envelopes provide the 95% confidence interval. All sample wells were modeled using only a single sample, with the exception of the R2ARD17 well in which two samples (R2ARD17-1 and R2ARD17-2) were modeled together, with a vertical offset distance of ~250 m. Regional geology has been considered in modeling of samples from the western Tennant region and northern Aileron Province (Green & Duddy, 2021), in which an unconformity between Proterozoic basement and the Wiso Basin and Georgina basin, respectively, has been used to constrain timing of close proximity to surface (Adelaide Resources Ltd., 2010; Ahmad & Munson, 2013; Chuck, 1982; Dunster et al., 2007; Menzies & Louwrens, 1995; Walter et al., 1989).

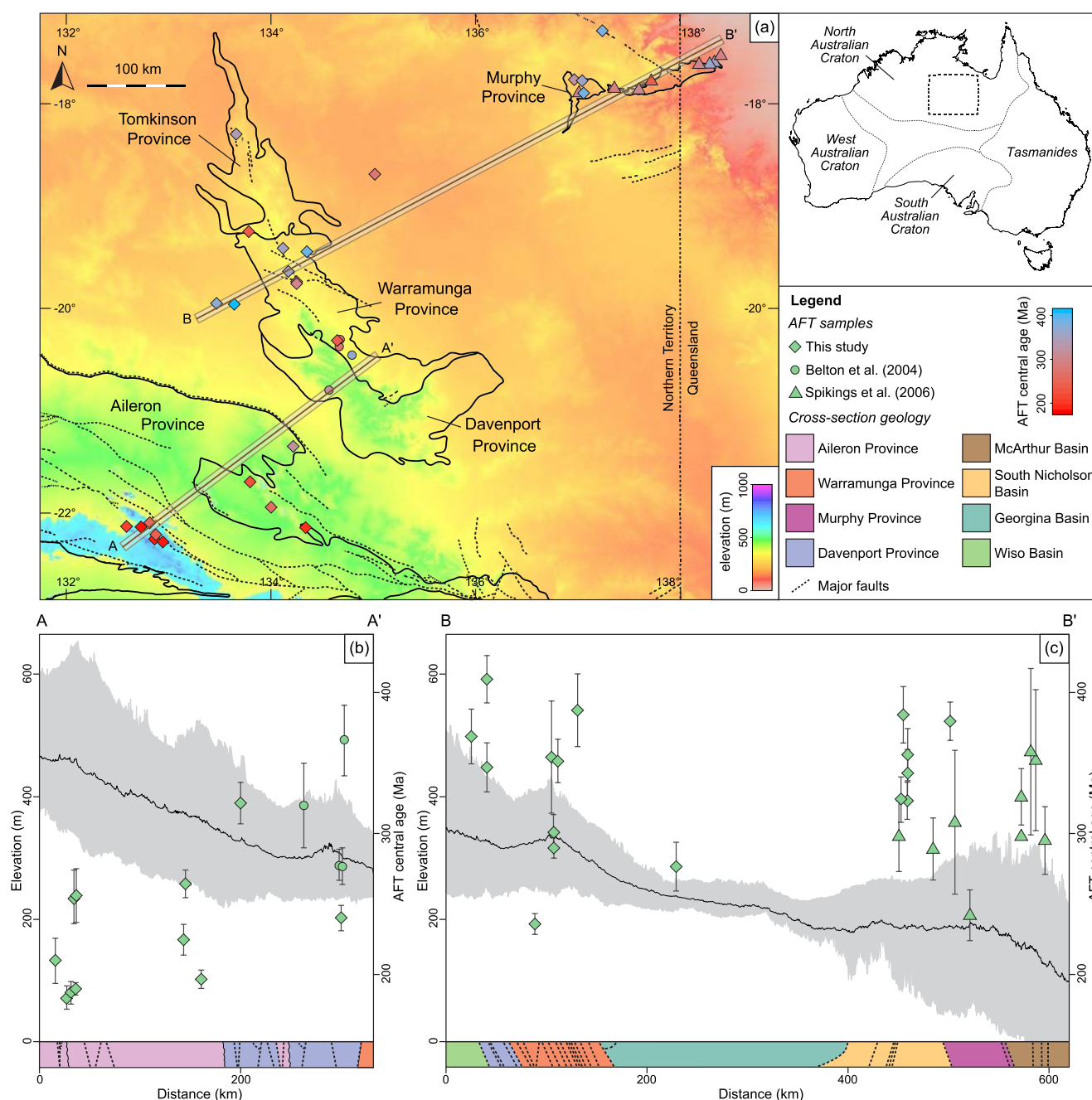


Figure 5. (a) Topographic map of central Australia showing major geological regions and locations of apatite fission track (AFT) samples. Topographic base map is from the Global Multi-resolution Terrain Elevation Data (GMTED) topographic imagery from Danielson and Gesch (2011). (b) Swath profile and regional structural cross-sections for transect A–A', with AFT central ages and 1σ error data overlain. (c) Swath profile and regional structural cross-sections for transect B–B', with AFT central ages and 1σ error data overlain. Swath profiles were produced using the SwathProfiler software on ArcGIS (Pérez-Peña et al., 2017) applied to GMTED topography data. Cross-sections were derived from structural interpretations of Grimes and Sweet (1979), Bureau of Mineral Resources (1982), Donnellan (2008), Donnellan and Johnstone (2004), Korsch et al. (2011), Kruse et al. (2010), Rawlings et al. (2008), and Ahmad and Wygralak (1989). AFT data from this study has been supplemented by other regional data from Belton et al. (2004) and Spikings et al. (2006).

450–400 Ma cooling event is most likely facilitated by fault reactivation during the ca. 450–440 Ma Rodin-gan Event of the Alice Springs Orogeny (Hand et al., 1999; Mawby et al., 1999; Scrimgeour & Raith, 2001; Shaw & Black, 1991) – coeval with the ca. 443–425 Ma Benambran Orogeny of the Tasmanides (Ali, 2010; Fergusson et al., 2005; Glen et al., 2007). Sample PCRD1-1, however, preserves a younger cooling event at ca. 300–270 Ma (Figure 4), attributed to fault reactivation in the latest stages of the Alice Springs Orogeny (Ahmad

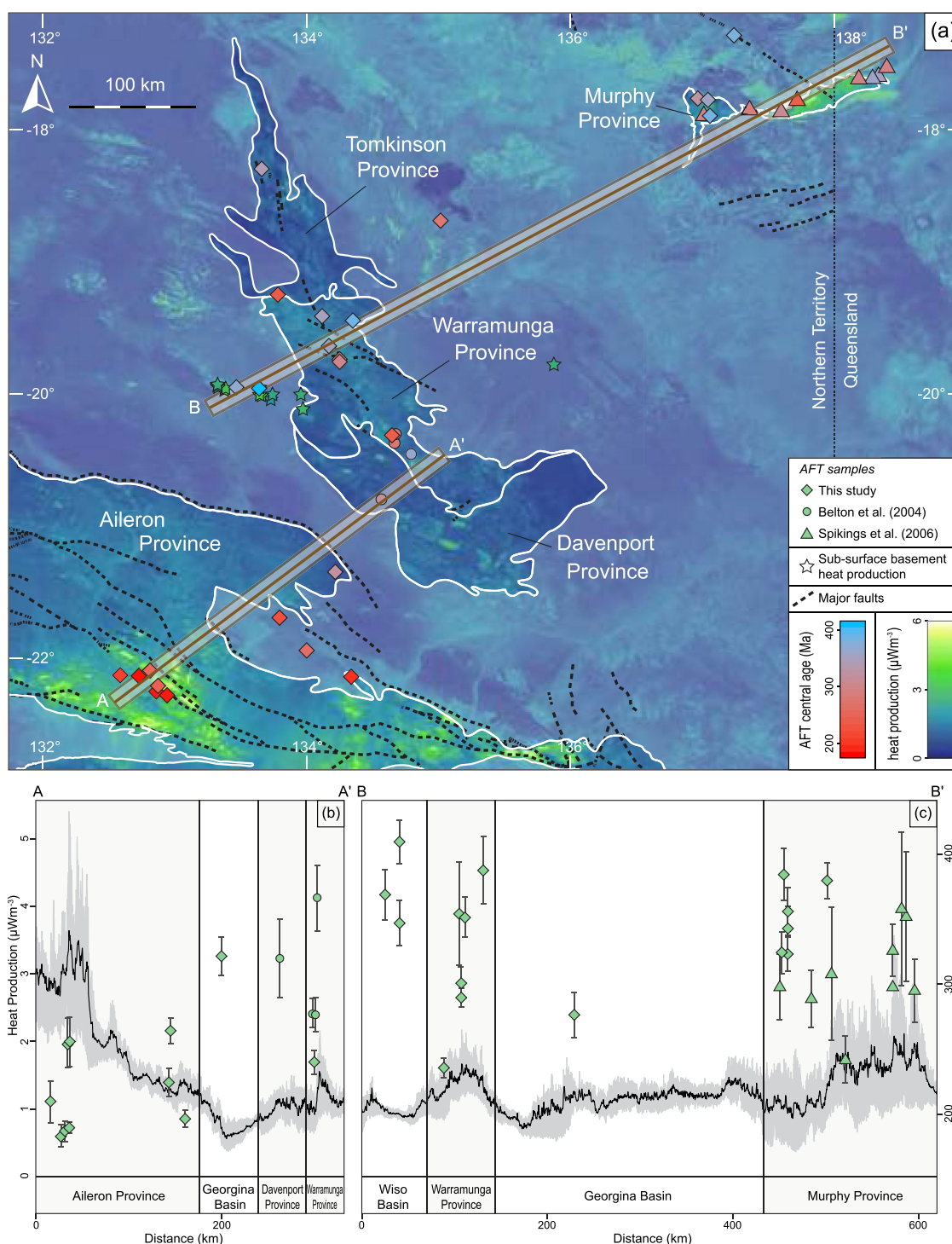


Figure 6.

& Munson, 2013; Bradshaw & Evans, 1988). The cooling profile of sample 2005080017 in the southern Warramunga Province (Figure 2) exhibits cooling spread between these two phases, and has most likely experienced multiple events during this period (Figure 4). The thermal history of the fault dominated Warramunga Province, therefore, likely experienced multiple fault reactivation events during the progression of the Alice Springs Orogeny (Figure 7), corresponding to vertical uplift of >1.4 km under a geothermal gradient of $\sim 28^\circ\text{C}/\text{km}$ (Holgate

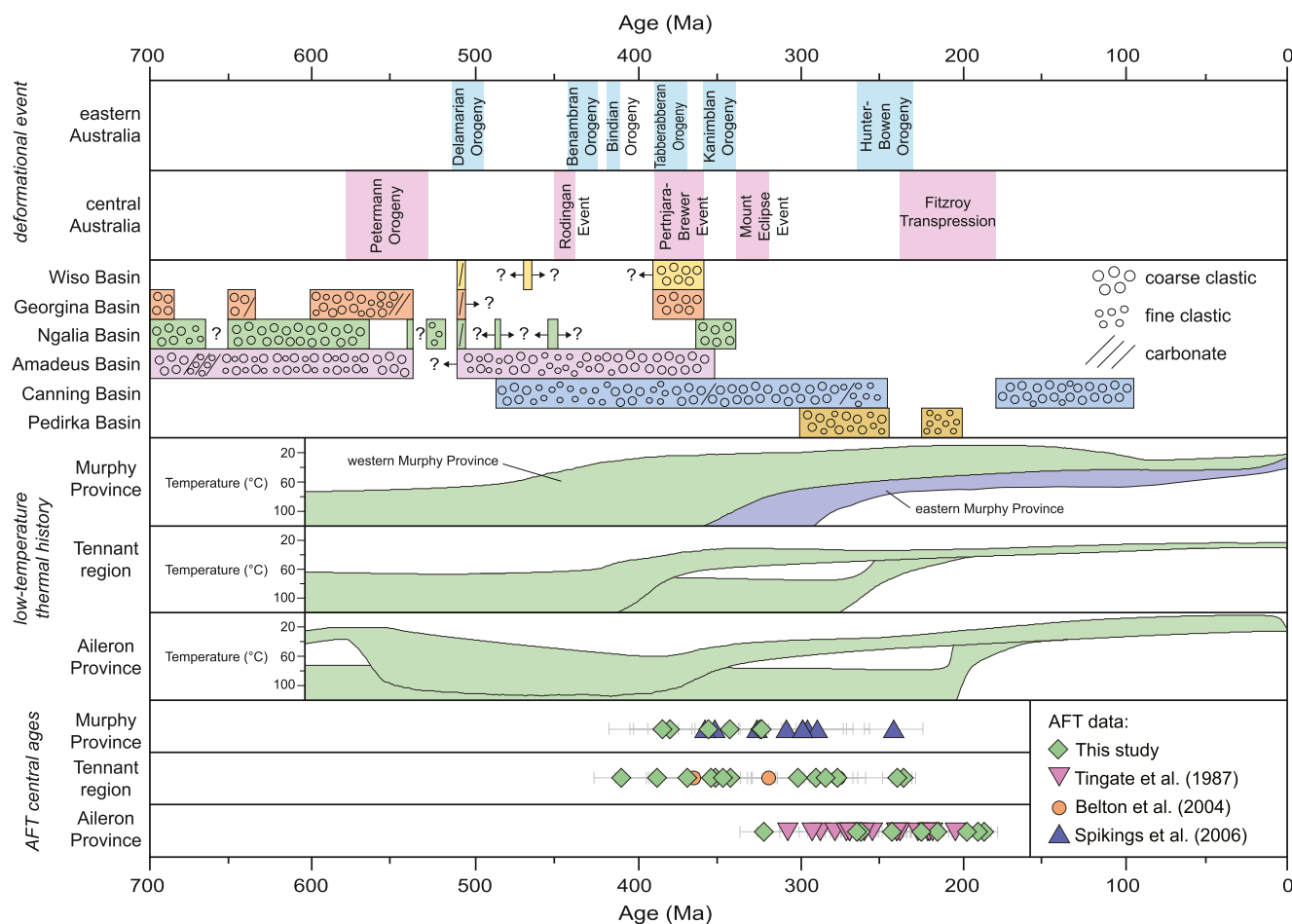


Figure 7. Time-space plot for the central North Australian Craton, depicting major deformational events, periods of sedimentation and low-temperature evolution (Ahmad & Munson, 2013; Aitken et al., 2009; Bradshaw & Evans, 1988; Hand & Sandiford, 1999; Hand et al., 1999; Horstman, 1984; Jones, 1972; Kennard et al., 1994; Mawby et al., 1999; Rosenbaum, 2018; Shaw & Black, 1991; Wade et al., 2005; Walter et al., 1995; Zhan & Mory, 2013). Generalized low-temperature thermal evolution models are from this study, with the exception of the eastern Murphy Province which is following Spikings et al. (2006). Regional apatite fission track central ages have been compiled from Belton et al. (2004), Spikings et al. (2006), and Tingate (1990).

& Gerner, 2010). This Paleozoic uplift has facilitated the exposure of mineralized Proterozoic basement to the surface (or near surface) at present day (Figure 1), exhuming it to feasible depths for extraction.

Samples on the western flank of the Warramunga Province, which is presently overlain by sedimentary rocks of the Wiso Basin (Donnellan, 2008; Donnellan et al., 2001), yield more consistent AFT ages and less abrupt thermal history profiles compared to the central Warramunga Province (Figure 5). In the western Warramunga Province, modeling of the R2ARD17 well suggests heating at ca. 520 Ma (Figure 4) as sediments of the Wiso Basin were deposited above the western extent of Warramunga Province basement. Following heating, the *Warramunga Formation* in the R2ARD17 well experienced cooling of ~30°C between ca. 450–350 Ma, most likely as

Figure 6. (a) Surface radiogenic heat production map of central Australia calculated at 250 Ma during the latter stages of Tasmanide deformation, following methodology of De Vries Van Leeuwen et al. (2021). Modern U, Th, and K abundances as determined by radiometric surveys (Minty et al., 2009, 2010) were extrapolated back in time based on respective isotopic decay constants to determine concentrations at 250 Ma, and transformed to radiogenic heat production using the expected heat production attributed to each element. Shaded areas denote basins which likely obscure more radiogenic underlying basement, hence heat production in these regions is likely to be vertically heterogeneous. Where possible, sub-surface basement heat production has additionally been calculated from average geochemistry of intersected crystalline rocks in drill holes NDIBK10, RVDD001, RVDD002, MXCURD001, MXCURD002, R27ARD18, R2ARD17, WGR3D001, TDD01, T3/2, 12BH002, 12BH003, WGR1D011, WGR1D003-1, WGR1D002, WGR1D034, WGR1D002-5, NR108D024, NR108D026, NR142D001, DDH 3, DDH 5, and DDH 4 (Geoscience Australia, 2022; Northern Territory Geological Survey, 2022), as shown by the stars. (b) Heat production and apatite fission track (AFT) central age data across transect A–A'. (c) Heat production and AFT central age data across transect B–B'. Heat production profiles were produced using the SwathProfiler software on ArcGIS (Pérez-Peña et al., 2017) applied to the radiogenic heat production map at 250 Ma in panel (a). AFT data from this study has been supplemented by other regional data from Belton et al. (2004) and Spikings et al. (2006).

a consequence of the subsequent erosion of ~ 1 km of overlying Wiso Basin sedimentary rocks under a geothermal gradient of $\sim 28^\circ\text{C}/\text{km}$ (Holgate & Gerner, 2010). It is most plausible that erosion was driven by uplift of the underlying Warramunga Province basement during the Alice Springs Orogeny (Ahmad & Munson, 2013; Bradshaw & Evans, 1988; Hand et al., 1999; Shaw & Black, 1991), synchronous with episodic fault reactivation experienced within the central Warramunga Province (Figures 5 and 7). Lack of major structural reactivation in this region, however, has resulted in erosion of considerably less overburden above Proterozoic basement than observed in the central Warramunga Province, which has hindered mineral exploration in this region.

The northern exposed Aileron Province preserves evidence of similar slow cooling associated with the removal of Neoproterozoic–Cambrian sedimentary rocks (Figure 4). Modeled drill holes from the northern Aileron Province (CMS3, DD94MG01, and RAQ278/DD1) predict an initial heating phase beginning at ca. 550 Ma as sedimentary rocks of the Centralian Superbasin (Georgina Basin) were deposited above rocks of the Aileron Province (Figure 4), followed by slow cooling of $\sim 30^\circ\text{C}$ between ca. 450–350 Ma, with denudation comparable to that proposed in the western Tennant region. This accelerated denudation was likely promoted by uplift of the northern Aileron Province during the Pertnjara-Brewer Event of the Alice Springs Orogeny (Ahmad & Munson, 2013; Bradshaw & Evans, 1988; Jones, 1972), which is itself coeval with the ca. 390–370 Ma Tabberabberan Orogeny of the Tasmanides (Black et al., 2005; Rosenbaum, 2018), where the northern Aileron Province was uplifted as foothills to the more heavily deformed central Aileron Province (e.g., Hand et al., 1999; Raimondo et al., 2012). While a genetic link between these events has not presently been established, strong temporal correlation suggest the possibility that stress generated at the eastern Australian margin may have influenced central Australia during the Alice Springs Orogeny (Raimondo et al., 2014).

Thermal history profiles in the Murphy Province similarly preserve cooling of $\sim 40^\circ\text{C}$ coeval with the Alice Springs Orogeny, although at a considerably slower rate than observed elsewhere in central Australia (Figure 4; Spikings et al., 2006). No apparent reactivation of structures is present across this region, with monotonic cooling attributed instead to slow exhumation of basement throughout the Ordovician–Carboniferous. Exhumation is contemporaneous with the ca. 390–360 Ma Pertnjara-Brewer Event of the Alice Springs Orogeny (Ahmad & Munson, 2013; Bradshaw & Evans, 1988; Jones, 1972), which is also observed in the Pine Creek Orogen (Nixon et al., 2021) and McArthur Basin (Nixon, Glorie, Hasterok, et al., 2022) in the NAC, and the Musgrave Province (Glorie, Agostino, et al., 2017; Quentin de Gromard et al., 2019) and Peake and Denison Inliers (Hall et al., 2016) in the northern South Australian Craton. Few favorably oriented major Proterozoic faults are observed within the Murphy Province, which has deprived the region of potential for significant differential exhumation and resulted in largely monotonic cooling profiles. Comparable slow cooling is also observed in the Arnhem Province (Nixon et al., 2021), which is similarly deficient in favourable structural crustal weaknesses.

Only a single sub-surface sample, BN04DD01-1, has been taken from the *Helen Springs Volcanics*, immediately underlying the Georgina Basin which overlies the Mesoproterozoic *Renner Group* of the Tomkinson Province to the east of the outcropping Warramunga Province (Kruse, 2008). An AFT central age of 277 ± 17 Ma has been obtained from limited grains from this sample ($n = 11$), although lack of a viable confined track distribution limits the potential for detailed interpretation. The most plausible scenario facilitating cooling during the Late-Paleozoic is denudational lag as sediments were slowly eroded following gentle exhumation of the region (e.g., Gleadow & Brown, 2000; Sueoka et al., 2012) during the Alice Springs Orogeny (Ahmad & Munson, 2013; Bradshaw & Evans, 1988; Raimondo et al., 2010), which terminated sedimentation in the Georgina Basin and drove erosion of the upper units. Similar slow cooling has been proposed in the McArthur Basin (Nixon, Glorie, Hasterok, et al., 2022), which further suggests a prevalence of slow, often lagging, cooling in sedimentary basins across the NAC during the Alice Springs Orogeny, with the majority of deformation and more immediate cooling focused in Proterozoic basement around pre-existing fault structures (Glorie, Agostino, et al., 2017; Hall et al., 2016, 2018; Nixon et al., 2021; Shaw & Black, 1991; Spikings et al., 2006).

5.2. Permian–Triassic

Low-temperature data from the eastern Murphy Province presented by Spikings et al. (2006) suggests cooling in this region persisted for notably longer than that observed in the western Murphy Province. Cooling in the eastern Murphy Province continued through ca. 300–250 Ma (Figure 7), where in the western Murphy Province no appreciable cooling is preserved beyond ca. 300 Ma (Figures 5 and 7). Permian cooling is additionally preserved further east in the Palaeoproterozoic Mount Isa Inlier, at the eastern edge of the NAC (Spikings et al., 1997).

This younger cooling progression is most likely linked to the inboard propagation of strain during the later stages of the Tasmanide accretion at the east Australian margin (Spikings et al., 1997, 2006), most likely during the Lachlan Orogeny and Hunter-Bowen Orogeny (e.g., Glen et al., 2009; Jessop et al., 2019; Rosenbaum, 2018). It is, however, notable that the exposed eastern Murphy Province appears to display elevated heat production (Figures 6a and 6c) corresponding to an elevated geothermal gradient estimated at $\sim 33^{\circ}\text{C}/\text{km}$ (Supporting Information S1), causing the lithosphere to become thermally weakened. Continued cooling during Tasmanide accretion observed only in the eastern Murphy Province was, therefore, a likely consequence of the closer proximity to the eastern Australian margin and comparatively weaker crustal strength. Cooling was slowed, however, due to the lack of easily reactivated crustal weaknesses (Ahmad & Wygralak, 1989; Rawlings et al., 2008), with cooling of $\sim 30^{\circ}\text{C}$ during the Permian (Spikings et al., 2006) indicative of ~ 0.9 km of exhumation.

The youngest cooling observed in this study is preserved within the Anmatjira Range of the central Aileron Province (Figures 5 and 6). The three modeled samples for this area, and the southernmost drill hole from the northern Aileron Province (CMS3) suggest the presence of a rapid cooling event at ca. 230–200 Ma (Figure 4). This cooling event occurs well after the recognized termination of the Alice Springs Orogeny *sensu stricto* at ca. 320 Ma, as determined by the occurrence of regional metamorphism (Ahmad & Munson, 2013; Bradshaw & Evans, 1988). Younger cooling histories in this region compared to that of the Tennant region are mirrored by an increase in local topography toward the southwest (Figures 5a and 5b), and are indicative of post-Carboniferous differential uplift between the two terranes, as separated by major northwest trending faults. Structural relationships in the Aileron Province suggest major east-west trending faults developed in the Proterozoic (Weisheit, 2019) and were reactivated during the Alice Springs Orogeny and subsequent events with reactivation characterized by brittle deformation of the upper crust (Reno et al., 2017, 2020).

The Aileron Province, and particularly the Anmatjira Range area, is typified by abnormally high crustal heat production (Figure 6), generated from highly radiogenic basement (Alessio et al., 2020; Anderson et al., 2013; Sandiford & Hand, 1998). Permian–Triassic crustal heat production in the Aileron Province (~ 6 to $4\ \mu\text{W m}^{-3}$; Figure 6) is significantly greater than that observed in the western Murphy Province (~ 2 to $1\ \mu\text{W m}^{-3}$; Figure 6) and sub-surface basement of the Warramunga Province (~ 3.5 to $2.5\ \mu\text{W m}^{-3}$; Figure 6), and notably higher than the global crustal average ($\sim 1\ \mu\text{W m}^{-3}$; e.g., Hasterok & Webb, 2017; McLennan & Taylor, 1996; Rudnick et al., 1998), which has produced a highly elevated regional geothermal gradient over time (e.g., Alessio et al., 2020; Anderson et al., 2013; Howlett et al., 2015; Morrissey et al., 2014). In addition, regional metasomatic alteration in this area, partially along shear-zones, has further weakened the crustal strength of the region (Raimondo et al., 2011). This combination of thermal lithospheric weakening and metasomatic alteration has promoted mechanically favorable conditions for structural reactivation within the Aileron Province, resulting in the localization of significant strain during the Alice Springs Orogeny (Hand & Sandiford, 1999; Raimondo et al., 2011, 2012; Sandiford & Hand, 1998), as well as renewed reactivation during the Triassic. This Triassic pulse of reactivation can be correlated to deformation in the far-field Hunter-Bowen Orogeny on the eastern Australian margin (ca. 265–230 Ma; Babaahmadi et al., 2017; Hoy & Rosenbaum, 2017; Roberts & Engel, 1987; Rosenbaum, 2018; Rosenbaum et al., 2012). In addition to the crustal weakening induced by high basement heat production, the elevated gradient would have required comparatively little overburden (~ 1.7 km) to be removed in order to completely cool through the APAZ, although this is still greater than that observed within the western Murphy Province during the Permian–Triassic. Hence, the combination of a high geothermal gradient and a weak crust in the Aileron Province has allowed subtler reactivation to be recorded by the AFT system in response to far-field tectonics at the eastern Australian margin. In sharp contrast, the more proximal but stronger Murphy Province does not record AFT evidence for widespread Triassic reactivation (Figures 4 and 6).

6. Conclusions

Palaeoproterozoic basement terranes that crop out within the central NAC demonstrate clear Paleozoic reactivation contemporaneous with multiple orogenic events driven by far-field plate boundary motions. Reactivation corresponding with the Late-Ordovician–Carboniferous Alice Springs Orogeny is observed in the Tennant region, Murphy Province and northern Aileron Province. The Tennant region underwent episodic fault reactivation during the Alice Springs Orogeny, facilitating faster cooling and denudation near shear-zones. Contemporaneous cooling is observed within the Murphy Province, although a lack of widespread pre-existing faults did not allow for rapid denudation and the region instead preserves a prolonged slow cooling profile. The central Aileron

Province experienced younger reactivation coeval with the Hunter-Bowen Orogeny at the eastern Australian margin, with local thermal and structural lithospheric weakening promoting preferential strain localization in this region. Hence, this study further supports a model of widespread Paleozoic deformation of the NAC as a response to forces generated at the eastern Gondwanan margin of Australia, with strain preferentially expressed through pre-existing structures within Proterozoic basement in response to orogenic events. Later deformation associated with the youngest orogenic events in eastern Australia (Hunter-Bowen Orogeny) is more localized, and confined to regions of highly weakened crust that is more susceptible to reactivation.

Data Availability Statement

Original data generated from this study are openly available on the Figshare platform (<https://doi.org/10.25909/635a082abfe40>), and previously published GIS data sets used in the elevation and heat production maps are available from the following references: Danielson and Gesch (2011), Geoscience Australia (2022), Minty et al. (2010), Minty et al. (2009), and Northern Territory Geological Survey (2022).

Acknowledgments

The authors wish to acknowledge the Aboriginal Traditional Owners of the land on which this work was carried out. The authors further wish to acknowledge Diana Zivak for assistance with sample preparation, and Sarah Gilbert and Benjamin Wade for aid with data collection. Samples CH11LJH171, 2006080003, 2005080048, 2005080045, 2005080017, 78063319, 78063318, and 78063317 were provided by Geoscience Australia, in collaboration with the Northern Territory Geological Survey. This work has been supported by the Mineral Exploration Cooperative Research Centre whose activities are funded by the Australian Government's Cooperative Research Centre Program. This is MinEx CRC Document 2022/78. Research was additionally funded by an Australian Research Council Linkage Projects (LP160101353 and LP200301457), which is partnered by the Northern Territory Geological Survey, SANTOS Ltd, Origin Energy, Teck Resources, CSIRO and Imperial Oil and Gas, and an Australian Research Council LIEF Project (LE150100145). Geoff Fraser publishes with the permission of the CEO, Geoscience Australia.

References

- Adelaide Resources Ltd. (2010). *Bringing forward discovery, geophysics and drilling collaboration – Drilling report, Rover project, SEL 27372* (CR2010-0326). Northern Territory Geological Survey. Retrieved from <https://geoscience.nt.gov.au/gemis/ntgsjspui/handle/1/75816>
- Ahmad, M., & Munson, T. J. (2013). *Geology and mineral resources of the Northern Territory* (Vol. Special Publication 5). Northern Territory Geological Survey.
- Ahmad, M., & Wygralak, A. S. (1989). *Calvert Hills, Northern Territory: Explanatory notes* (SE 53-08). Northern Territory Geological Survey. Retrieved from <https://geoscience.nt.gov.au/gemis/ntgsjspui/handle/1/81915>
- Aitken, A. R. A., Betts, P. G., & Ailleres, L. (2009). The architecture, kinematics, and lithospheric processes of a compressional intraplate orogen occurring under Gondwana assembly: The Petermann orogeny, central Australia. *Lithosphere*, 1(6), 343–357. <https://doi.org/10.1130/L39.1>
- Alessio, K. L., Hand, M., Hasterok, D., Morrissey, L. J., Kelsey, D. E., & Raimondo, T. (2020). Thermal modelling of very long-lived (>140 Myr) high thermal gradient metamorphism as a result of radiogenic heating in the Reynolds Range, central Australia. *Lithos*, 352–353, 105280. <https://doi.org/10.1016/j.lithos.2019.105280>
- Ali, A. (2010). The tectono-metamorphic evolution of the Balcooma Metamorphic Group, north-eastern Australia: A multidisciplinary approach. *Journal of Metamorphic Geology*, 28(4), 397–422. <https://doi.org/10.1111/j.1525-1314.2010.00871.x>
- Anderson, J. R., Kelsey, D. E., Hand, M., & Collins, W. J. (2013). Conductively driven, high-thermal gradient metamorphism in the Anmatjira Range, Arunta region, central Australia. *Journal of Metamorphic Geology*, 31(9), 1003–1026. <https://doi.org/10.1111/jmg.12054>
- Babaahmadi, A., Sliwa, R., Esterle, J., & Rosenbaum, G. (2017). The development of a Triassic fold-thrust belt in a synclinal depositional system, Bowen Basin (eastern Australia). *Tectonics*, 36(1), 51–77. <https://doi.org/10.1002/2016TC004297>
- Belton, D. X., Brown, R. W., Kohn, B. P., Fink, D., & Farley, K. A. (2004). Quantitative resolution of the debate over antiquity of the central Australian landscape: Implications for the tectonic and geomorphic stability of cratonic interiors. *Earth and Planetary Science Letters*, 219(1), 21–34. [https://doi.org/10.1016/S0012-821X\(03\)00705-2](https://doi.org/10.1016/S0012-821X(03)00705-2)
- Black, L. P. (1984). U-Pb zircon ages and a revised chronology for the Tennant Creek Inlier, Northern Territory. *Australian Journal of Earth Sciences*, 31(1), 123–131. <https://doi.org/10.1080/08120098408729284>
- Black, L. P., McClenaghan, M. P., Korsch, R. J., Everard, J. L., & Foudoulis, C. (2005). Significance of Devonian–Carboniferous igneous activity in Tasmania as derived from U–Pb SHRIMP dating of zircon. *Australian Journal of Earth Sciences*, 52(6), 807–829. <https://doi.org/10.1080/08120090500304232>
- Boger, S. D., & Miller, J. M. (2004). Terminal suturing of Gondwana and the onset of the Ross–Delamerian Orogeny: The cause and effect of an Early Cambrian reconfiguration of plate motions. *Earth and Planetary Science Letters*, 219(1), 35–48. [https://doi.org/10.1016/S0012-821X\(03\)00692-7](https://doi.org/10.1016/S0012-821X(03)00692-7)
- Bradshaw, J. D., & Evans, P. R. (1988). Palaeozoic tectonics, Amadeus Basin, central Australia. *The APPEA Journal*, 28(1), 267–282. <https://doi.org/10.1071/AJ87021>
- Bureau of Mineral Resources. (1982). *Napperby, Northern Territory: Sheet SF5309* (SF 53-09). Northern Territory Geological Survey. Retrieved from <https://geoscience.nt.gov.au/gemis/ntgsjspui/handle/1/81703>
- Carlson, W. D., Donelick, R. A., & Ketcham, R. A. (1999). Variability of apatite fission-track annealing kinetics: I. Experimental results. *American Mineralogist*, 84(9), 1213–1223. <https://doi.org/10.2138/am-1999-0901>
- Carson, C. J., Hollis, J. A., Glass, L. M., Close, D. F., Whelan, J. A., & Wygralak, A. S. (2011). *Summary of results. Joint NTGS-GA geochronology project: Pine Creek Orogen, eastern Arunta region, Murphy inlier and Amadeus Basin, July 2007–June 2009* (NTGS Record 2010-004). Northern Territory Geological Survey. Retrieved from <https://geoscience.nt.gov.au/gemis/ntgsjspui/handle/1/82453>
- Cawood, P. A., & Korsch, R. J. (2008). Assembling Australia: Proterozoic building of a continent. *Precambrian Research*, 166(1–4), 1–35. <https://doi.org/10.1016/j.precamres.2008.08.006>
- Chew, D. M., Babechuk, M. G., Cogné, N., Mark, C., O'Sullivan, G. J., Henrichs, I. A., et al. (2016). (LA, Q)-ICPMS trace-element analyses of Durango and McClure Mountain apatite and implications for making natural LA-ICPMS mineral standards. *Chemical Geology*, 435, 35–48. <https://doi.org/10.1016/j.chemgeo.2016.03.028>
- Chuck, R. G. (1982). *Annual report for EL2654, Mount Skinner, NT, for the period 24/1/81–23/1/82* (CR1982-0183). Northern Territory Geological Survey. Retrieved from <https://geoscience.nt.gov.au/gemis/ntgsjspui/handle/1/60912>
- Clauoué-Long, J., Edgoose, C. J., & Worden, K. (2008). A correlation of Aileron Province stratigraphy in central Australia. *Precambrian Research*, 166(1), 230–245. <https://doi.org/10.1016/j.precamres.2007.06.022>
- Clauoué-Long, J., Maidment, D., & Donnellan, N. (2008). Stratigraphic timing constraints in the Davenport Province, central Australia: A basis for Palaeoproterozoic correlations. *Precambrian Research*, 166(1), 204–218. <https://doi.org/10.1016/j.precamres.2007.06.021>
- Close, D., Scrimgeour, I., Carson, C., & Clauoué-Long, J. (2007). Diverse terranes and mineral potential of the Casey Inlier, Arunta region. *Paper presented at the Annual Geoscience Exploration Seminar (AGES) 2007, Alice Springs, Northern Territory*.

- Close, D. F. (2014). The McArthur Basin: NTGS' approach to a Frontier petroleum basin with known base metal prospectivity. *Paper presented at the Annual Geoscience Exploration Seminar (AGES), Alice Springs, NT.*
- Compston, D. M. (1995). Time constraints on the evolution of the Tennant Creek Block, northern Australia. *Precambrian Research*, 71(1), 107–129. [https://doi.org/10.1016/0301-9268\(94\)00058-Y](https://doi.org/10.1016/0301-9268(94)00058-Y)
- Compston, D. M., & McDougall, I. (1994). ^{40}Ar - ^{39}Ar and K-Ar age constraints on the Early Proterozoic Tennant Creek Block, northern Australia, and the age of its gold deposits. *Australian Journal of Earth Sciences*, 41(6), 609–616. <https://doi.org/10.1080/08120099408728171>
- Coney, P. J., Edwards, A., Hine, R., Morrison, F., & Windrim, D. (1990). The regional tectonics of the Tasman orogenic system, eastern Australia. *Journal of Structural Geology*, 12(5), 519–543. [https://doi.org/10.1016/0191-8141\(90\)90071-6](https://doi.org/10.1016/0191-8141(90)90071-6)
- Cross, A. J., Clark, A. D., Schofield, A., & Kositcin, N. (2020). New SHRIMP U–Pb zircon and monazite geochronology of the East Tennant region: A possible undercover extension of the Warramunga Province, Tennant Creek. Geoscience Australia.
- Danielson, J. J., & Gesch, D. B. (2011). *Global multi-resolution terrain elevation data 2010 (GMTED2010)* (2011-1073). U. S. Geological Survey. Retrieved from <http://pubs.er.usgs.gov/publication/ofr20111073>
- De Vries Van Leeuwen, A. T., Hand, M., Morrissey, L. J., & Raimondo, T. (2021). Th–U powered metamorphism: Thermal consequences of a chemical hotspot. *Journal of Metamorphic Geology*, 39(5), 541–565. <https://doi.org/10.1111/jmg.12590>
- Donelick, R. A., & Miller, D. S. (1991). Enhanced TINT fission-track densities in low spontaneous track density apatites using ^{252}Cf -derived fission fragment tracks: A model and experimental observations. *Nuclear Tracks and Radiation Measurements*, 18(3), 301–307. [https://doi.org/10.1016/1359-0189\(91\)90022-a](https://doi.org/10.1016/1359-0189(91)90022-a)
- Donnellan, N. C. (2008). *Mount Peake – Lander river, Northern Territory: combined explanatory notes* (SF 53-05, SF 53-01, pp. 1–85). Northern Territory Geological Survey. Retrieved from <https://geoscience.nt.gov.au/gemis/ntgsjspsui/handle/1/81867>
- Donnellan, N. C., Hussey, K. J., & Morrison, R. S. (1995). *Flynn – Tennant Creek, Northern Territory: Combined explanatory notes* (5759, 5759, pp. 1–79). Northern Territory Geological Survey. Retrieved from <https://geoscience.nt.gov.au/gemis/ntgsjspsui/handle/1/81868>
- Donnellan, N. C., & Johnstone, A. (2004). *Mapped and interpreted geology of the Tennant Region 1:500 000 scale*. Northern Territory Geological Survey. Retrieved from <https://geoscience.nt.gov.au/gemis/ntgsjspsui/handle/1/82053>
- Donnellan, N. C., Morrison, R. S., Hussey, K. J., Ferenczi, P. A., & Kruse, P. D. (2001). *Tennant Creek, Northern Territory: Explanatory notes* (SE 53-14, pp. 1–54). Northern Territory Geological Survey. Retrieved from <https://geoscience.nt.gov.au/gemis/ntgsjspsui/handle/1/81871>
- Dunster, J. N., Kruse, P. D., Duffett, M. L., & Ambrose, G. J. (2007). *Geology and resource potential of the southern Georgina Basin (DIP007, pp. 1–232)*. Northern Territory Geological Survey. Retrieved from <https://geoscience.nt.gov.au/gemis/ntgsjspsui/handle/1/81746>
- Fergusson, C. L., Fanning, C. M., Phillips, D., & Ackerman, B. R. (2005). Structure, detrital zircon U–Pb ages and $^{40}\text{Ar}/^{39}\text{Ar}$ geochronology of the Early Palaeozoic Girilambone Group, central New South Wales: Subduction, contraction and extension associated with the Benambran Orogeny. *Australian Journal of Earth Sciences*, 52(1), 137–159. <https://doi.org/10.1080/08120090500100044>
- Foden, J., Elburg, M. A., Dougherty-Page, J., & Burt, A. (2006). The timing and duration of the Delamerian Orogeny: Correlation with the Ross Orogen and implications for Gondwana assembly. *The Journal of Geology*, 114(2), 189–210. <https://doi.org/10.1086/499570>
- Fraser, G. L., Hussey, K., & Compston, D. M. (2008). Timing of palaeoproterozoic Au–Cu–Bi and W-mineralization in the Tennant Creek region, northern Australia: Improved constraints via intercalibration of $^{40}\text{Ar}/^{39}\text{Ar}$ and U–Pb ages. *Precambrian Research*, 164(1), 50–65. <https://doi.org/10.1016/j.precamres.2008.03.005>
- Gallagher, K. (2012). Transdimensional inverse thermal history modeling for quantitative thermochronology. *Journal of Geophysical Research*, 117(B2), 1–16. <https://doi.org/10.1029/2011jb008825>
- Gard, M., Hasterok, D., Hand, M., & Cox, G. (2019). Variations in continental heat production from 4 Ga to the present: Evidence from geochemical data. *Lithos*, 342–343, 391–406. <https://doi.org/10.1016/j.lithos.2019.05.034>
- Geoscience Australia. (2022). *East Tennant whole rock inorganic geochemistry data release*. Geoscience Australia. Retrieved from <https://ecat.ga.gov.au/geonetwork/srv/eng/catalog.search%23/metadata/146418>
- Gleadow, A. J. W., & Brown, R. W. (2000). Fission-track thermochronology and the long-term denudational response to tectonics. In M. A. Summerfield (Ed.), *Geomorphology and global tectonics* (pp. 57–75). John Wiley & Sons.
- Gleadow, A. J. W., Duddy, I. R., Green, P. F., & Lovering, J. F. (1986). Confined fission track lengths in apatite: A diagnostic tool for thermal history analysis. *Contributions to Mineralogy and Petrology*, 94(4), 405–415. <https://doi.org/10.1007/bf00376334>
- Glen, R. A., Meffre, S., & Scott, R. J. (2007). Benambran Orogeny in the Eastern Lachlan Orogen, Australia. *Australian Journal of Earth Sciences*, 54(2–3), 385–415. <https://doi.org/10.1080/08120090601147019>
- Glen, R. A., Percival, I. G., & Quinn, C. D. (2009). Ordovician continental margin terranes in the Lachlan Orogen, Australia: Implications for tectonics in an accretionary orogen along the east Gondwana margin. *Tectonics*, 28(6), TC6012. <https://doi.org/10.1029/2009tc002446>
- Glorie, S., Agostino, K., Dutch, R., Pawley, M., Hall, J., Danišik, M., et al. (2017). Thermal history and differential exhumation across the Eastern Musgrave Province, South Australia: Insights from low-temperature thermochronology. *Tectonophysics*, 703–704, 23–41. <https://doi.org/10.1016/j.tecto.2017.03.003>
- Glorie, S., Alexandrov, I., Nixon, A., Jepson, G., Gillespie, J., & Jahn, B. M. (2017). Thermal and exhumation history of Sakhalin Island (Russia) constrained by apatite U–Pb and fission track thermochronology. *Journal of Asian Earth Sciences*, 143, 326–342. <https://doi.org/10.1016/j.jseaes.2017.05.011>
- Glorie, S., Hall, J. W., Nixon, A., Collins, A. S., & Reid, A. (2019). Carboniferous fault reactivation at the northern margin of the metal-rich Gawler Craton (South Australia): Implications for ore deposit exhumation and preservation. *Ore Geology Reviews*, 115, 103193. <https://doi.org/10.1016/j.oregeorev.2019.103193>
- Green, P. F., & Duddy, I. R. (2021). Discussion: Extracting thermal history from low temperature thermochronology. A comment on recent exchanges between Vermeesch and Tian and Gallagher and Ketcham. *Earth-Science Reviews*, 216, 103197. <https://doi.org/10.1016/j.earscirev.2020.103197>
- Grimes, K. G., & Sweet, I. P. (1979). *Explanatory notes on the Westmoreland geological sheet (second edition)* (SE54-05, pp. 1–31). Geological Survey of Queensland. Retrieved from <https://geoscience.data.qld.gov.au/dataset/mr000434/resource/0bde30ad-8d07-4e54-90d3-e64bf7644ee4>
- Haines, P. W. (1991). *Barrow Creek, Northern Territory: Explanatory notes* (SF 53-6, pp. 1–53). Northern Territory Geological Survey. Retrieved from <https://geoscience.nt.gov.au/gemis/ntgsjspsui/handle/1/81883>
- Haines, P. W., Hand, M., & Sandiford, M. (2001). Palaeozoic synorogenic sedimentation in central and northern Australia: A review of distribution and timing with implications for the evolution of intracontinental orogens. *Australian Journal of Earth Sciences*, 48(6), 911–928. <https://doi.org/10.1046/j.1440-0952.2001.00909.x>
- Hall, J. W., Glorie, S., Collins, A. S., Reid, A., Evans, N., McInnes, B., & Foden, J. (2016). Exhumation history of the Peake and Denison Inliers: Insights from low-temperature thermochronology. *Australian Journal of Earth Sciences*, 63(7), 805–820. <https://doi.org/10.1080/08120099.2016.1253615>

- Hall, J. W., Glorie, S., Reid, A. J., Collins, A. S., Jourdan, F., Danišik, M., & Evans, N. (2018). Thermal history of the northern Olympic Domain, Gawler Craton: correlations between thermochronometric data and mineralising systems. *Gondwana Research*, 56, 90–104. <https://doi.org/10.1016/j.gr.2018.01.001>
- Hand, M., Mawby, J., Miller, J. A., Ballevre, M., Hensen, B. J., Moller, A., & Buick, I. S. (1999). Tectonothermal evolution of the Harts and Strangways range region, eastern Arunta inlier, central Australia, Specialist Group in Geochemistry, Mineralogy and Petrology, (*Field Guide* 4).
- Hand, M., & Sandiford, M. (1999). Intraplate deformation in central Australia, the link between subsidence and fault reactivation. *Tectonophysics*, 305(1), 121–140. [https://doi.org/10.1016/S0040-1951\(99\)00009-8](https://doi.org/10.1016/S0040-1951(99)00009-8)
- Hasterok, D., & Gard, M. (2016). Utilizing thermal isostasy to estimate sub-lithospheric heat flow and anomalous crustal radioactivity. *Earth and Planetary Science Letters*, 450, 197–207. <https://doi.org/10.1016/j.epsl.2016.06.037>
- Hasterok, D., & Webb, J. (2017). On the radiogenic heat production of igneous rocks. *Geoscience Frontiers*, 8(5), 919–940. <https://doi.org/10.1016/j.gsf.2017.03.006>
- Hoatson, D. M., Sun, S.-S., & Clauoué-Long, J. C. (2005). Proterozoic mafic-ultramafic intrusions in the Arunta region, central Australia: Part 1: Geological setting and mineral potential. *Precambrian Research*, 142(3), 93–133. <https://doi.org/10.1016/j.precamres.2005.09.004>
- Holgate, F. L., & Gerner, E. J. (2010). *OZTemp well temperature data*. Geoscience Australia. Retrieved from <https://pid.geoscience.gov.au/data-set/ga/70604https://researchdata.edu.au/oztemp-well-temperature-data>
- Hollis, J. A., Beyer, E. E., Whelan, J. A., Kemp, A. I. S., Scherst, N. A., & Greig, A. (2010). *Summary of results. NTGS laser U-Pb and Hf geochronology project: Pine Creek Orogen, Murphy Inlier, McArthur Basin and Arunta region, July 2007–May 2008* (NTGS Record 2010-001). Northern Territory Geological Survey. Retrieved from <https://geoscience.nt.gov.au/gemis/ntgsjspui/handle/1/82451>
- Horstman, E. L. (1984). Evidence for post-Permian epeirogenic uplift in the Canning Basin from vitrinite reflectance data. In P. G. Purcell (Ed.), *The Canning Basin* (pp. 401–409). Petroleum Exploration Society of Australia (PESA).
- Howlett, D., Raimondo, T., & Hand, M. (2015). Evidence for 1808–1770 Ma bimodal magmatism, sedimentation, high-temperature deformation and metamorphism in the Aileron Province, central Australia. *Australian Journal of Earth Sciences*, 62(7), 831–852. <https://doi.org/10.1080/08120099.2015.1108364>
- Hoy, D., & Rosenbaum, G. (2017). Episodic behavior of Gondwanide deformation in eastern Australia: Insights from the Gympie terrane. *Tectonics*, 36(8), 1497–1520. <https://doi.org/10.1002/2017TC004491>
- Hussey, K. J., Beier, P. R., Crispe, A. J., Donnellan, N., & Kruse, P. D. (2001). *Helen Springs, Northern Territory: Explanatory notes* (pp. 1–63). Northern Territory Geological Survey. Retrieved from <https://geoscience.nt.gov.au/gemis/ntgsjspui/handle/1/81888>
- Jenkins, R. J. F., & Sandiford, M. (1992). Observations on the tectonic evolution of the southern Adelaide Fold Belt. *Tectonophysics*, 214(1), 27–36. [https://doi.org/10.1016/0040-1951\(92\)90188-C](https://doi.org/10.1016/0040-1951(92)90188-C)
- Jessop, K., Daczko, N. R., & Piaolo, S. (2019). Tectonic cycles of the New England Orogen, eastern Australia: A review. *Australian Journal of Earth Sciences*, 66(4), 459–496. <https://doi.org/10.1080/08120099.2018.1548378>
- Jones, B. G. (1972). Upper Devonian to lower Carboniferous stratigraphy of the Pertnjara Group, Amadeus Basin, central Australia. *Journal of the Geological Society of Australia*, 19(2), 229–249. <https://doi.org/10.1080/14400957208527885>
- Kennard, J. M., Jackson, M. J., Romine, K. K., Shaw, R. D., & Southgate, P. N. (1994). Depositional sequences and associated petroleum systems of the Canning Basin, WA. *Paper presented at the The Sedimentary Basins of Western Australia, Perth, Western Australia*.
- Kennewell, P. J., & Huleatt, M. B. (1980). *Geology of the Wiso Basin, Northern Territory*. Bulletin 205, Bureau of Mineral Resources.
- Ketcham, R. A., Donelick, R. A., & Carlson, W. D. (1999). Variability of apatite fission-track annealing kinetics: III. Extrapolation to geological time scales. *American Mineralogist*, 84(9), 1235–1255. <https://doi.org/10.2138/am-1999-0903>
- Korsch, R. J., Blewett, R., Close, D. F., Scrimgeour, I. R., Huston, D. L., Kositsin, N., et al. (2011). Geological interpretation and geodynamic implications of the deep seismic reflection and magnetotelluric line 09GA-GA1: Georgina-Arunta Region, Northern Territory. *Paper presented at the Annual Geoscience Exploration Seminar (AGES) 2011, Alice Springs, Northern Territory*. Retrieved from <https://geoscience.nt.gov.au/gemis/ntgsjspui/handle/1/82296>
- Kositsin, N., Beyer, E. E., Whelan, J. A., Close, D. F., Hallett, L., & Dunkley, D. J. (2013). *Summary of results. Joint NTGS-GA geochronology project: Arunta region, Ngalia Basin, Tanami region and Murphy Province July 2011–June 2012* (NTGS Record 2013-004). Northern Territory Geological Survey. Retrieved from <https://geoscience.nt.gov.au/gemis/ntgsjspui/handle/1/82463>
- Kruse, P. D. (1998). *Cambrian palaeontology of the eastern Wiso and western Georgina Basins* (NTGS Report 9, pp. 1–68). Northern Territory Geological Survey. Retrieved from <https://geoscience.nt.gov.au/gemis/ntgsjspui/handle/1/81565>
- Kruse, P. D. (2008). *Georgina Basin stratigraphic drilling 2002–2006 and petrography 2000–2007* (NTGS Record 2008-001). Northern Territory Geological Survey. Retrieved from <https://geoscience.nt.gov.au/gemis/ntgsjspui/handle/1/82445>
- Kruse, P. D., Maier, R. C., Khan, M., & Dunster, J. N. (2010). *Walhallow – Brunette Downs – Alroy – Frew River, Northern Territory: Combined explanatory notes* (p. 69). Northern Territory Geological Survey. Retrieved from <https://geoscience.nt.gov.au/gemis/ntgsjspui/handle/1/81890>
- Li, P. F., Rosenbaum, G., & Rubatto, D. (2012). Triassic asymmetric subduction rollback in the southern New England Orogen (eastern Australia): The end of the Hunter-Bowen Orogeny. *Australian Journal of Earth Sciences*, 59(6), 965–981. <https://doi.org/10.1080/08120099.2012.696556>
- Maidment, D. W. (2013b). Sample 2005080049 (Warramunga Formation). Geoscience Australia OZCHRON geochronology database. Retrieved from <http://www.ga.gov.au/geochron-sapub-web/geochronology/shrimp/search.htm>
- Maidment, D. W., Huston, D. L., Donnellan, N., & Lambeck, A. (2013). Constraints on the timing of the Tennant Event and associated Au–Cu–Bi mineralisation in the Tennant region, Northern Territory. *Precambrian Research*, 237, 51–63. <https://doi.org/10.1016/j.precamres.2013.07.020>
- Maidment, D. W., Lambeck, L., Huston, D. L., & Donnellan, N. C. (2006). New geochronological data from the Tennant region. *Paper presented at the Annual Geoscience Exploration Seminar (AGES) 2006, Alice Springs, Northern Territory*. Retrieved from <https://geoscience.nt.gov.au/gemis/ntgsjspui/handle/1/82206>
- Marks, M. A. W., Wenzel, T., Whitehouse, M. J., Loose, M., Zack, T., Barth, M., et al. (2012). The volatile inventory (F, Cl, Br, S, C) of magmatic apatite: An integrated analytical approach. *Chemical Geology*, 291, 241–255. <https://doi.org/10.1016/j.chemgeo.2011.10.026>
- Mawby, J., Hand, M., & Foden, J. (1999). Sm–Nd evidence for high grade Ordovician metamorphism in the Arunta Block, Central Australia. *Journal of Metamorphic Geology*, 17(6), 653–668. <https://doi.org/10.1046/j.1525-1314.1999.00224.x>
- McDannell, K. T. (2020). *Notes on statistical age dispersion in fission-track datasets: The chi-square test, annealing variability, and analytical considerations*. EarthArXiv.
- McDannell, K. T., Schneider, D. A., Zeitler, P. K., O'Sullivan, P. B., & Issler, D. R. (2019). Reconstructing deep-time histories from integrated thermochronology: An example from southern Baffin Island, Canada. *Terra Nova*, 31(3), 189–204. <https://doi.org/10.1111/ter.12386>
- McDowell, F. W., McIntosh, W. C., & Farley, K. A. (2005). A precise ⁴⁰Ar–³⁹Ar reference age for the Durango apatite (U–Th)/He and fission-track dating standard. *Chemical Geology*, 214(3–4), 249–263. <https://doi.org/10.1016/j.chemgeo.2004.10.002>

- McLaren, S., Sandiford, M., Hand, M., Neumann, N. L., Wyborn, L. A. I., & Bastrakova, I. (2003). The hot southern continent: Heat flow production in Australian Proterozoic terranes. In R. R. Hillis & R. D. Muller (Eds.), *Evolution and dynamics of the Australian Plate* (Vol. 22, pp. 151–161). Geological Society of Australia.
- McLennan, S. M., & Taylor, S. R. (1996). Heat flow and the chemical composition of continental crust. *The Journal of Geology*, 104(4), 369–377. <https://doi.org/10.1086/629834>
- Menzies, D. C., & Louwrens, D. J. (1995). *EL 8016 Mount Gwynne and EL 8017 Mollie Bluff (N.T.), final report and annual report for period ending 27 April 1995* (CR1995-0562). Northern Territory Geological Survey. Retrieved from <https://geoscience.nt.gov.au/gemis/ntgsjspui/handle/1/62904>
- Minty, B. R. S., Franklin, R., Milligan, P. R., & Richardson, L. M. (2010). *Radiometric map of Australia* (2nd ed.). Geoscience Australia. Retrieved from <https://data.gov.au/dataset/ds-ga-a05f7892-f8c2-7506-e044-00144fdd4fa6/details?q=>
- Minty, B. R. S., Franklin, R., Milligan, P. R., Richardson, M., & Wilford, J. (2009). The radiometric map of Australia. *Exploration Geophysics*, 40(4), 325–333. <https://doi.org/10.1071/EG09025>
- Morrissey, L. J., Hand, M., Raimondo, T., & Kelsey, D. E. (2014). Long-lived high-T, low-P granulite facies metamorphism in the Arunta Region, central Australia. *Journal of Metamorphic Geology*, 32(1), 25–47. <https://doi.org/10.1111/jmg.12056>
- Nixon, A. L., Glorie, S., Collins, A. S., Blades, M. L., Simpson, A., & Whelan, J. A. (2022). Inter-cratonic geochronological and geochemical correlations of the Derim Derim–Galiwinku/Yanliao reconstructed Large Igneous Province across the North Australian and North China cratons. *Gondwana Research*, 103, 473–486. <https://doi.org/10.1016/j.gr.2021.10.027>
- Nixon, A. L., Glorie, S., Collins, A. S., Whelan, J. A., Reno, B. L., Danišik, M., et al. (2021). Footprints of the Alice Springs Orogeny preserved in far northern Australia: An application of multi-kinetic thermochronology in the Pine Creek Orogen and Arnhem Province. *Journal of the Geological Society*, 178(2), jgs2020-2173. <https://doi.org/10.1144/jgs2020-173>
- Nixon, A. L., Glorie, S., Hasterok, D., Collins, A. S., Fernie, N., & Fraser, G. (2022). Low-temperature thermal history of the McArthur Basin: Influence of the Cambrian Kalkarindji Large Igneous Province on hydrocarbon maturation. *Basin Research*. <https://doi.org/10.1111/bre.12691>
- Northern Territory Geological Survey. (1983). *Alice Springs – Darwin railway investigation: Geology* (GS1983-012). Northern Territory Geological Survey. Retrieved from <https://geoscience.nt.gov.au/gemis/ntgsjspui/handle/1/85651>
- Northern Territory Geological Survey. (2022). *Northern Territory geochemical datasets* (DIP001). Northern Territory Geological Survey. Retrieved from <https://geoscience.nt.gov.au/gemis/ntgsjspui/handle/1/81743>
- O'Sullivan, P. B., & Parrish, R. R. (1995). The importance of apatite composition and single-grain ages when interpreting fission track data from plutonic rocks: A case study from the Coast Ranges, British Columbia. *Earth and Planetary Science Letters*, 132(1), 213–224. [https://doi.org/10.1016/0012-821X\(95\)00058-K](https://doi.org/10.1016/0012-821X(95)00058-K)
- Page, R. W. (1996b). Sample 92-295 (Warramunga Formation). Geoscience Australia OZCHRON geochronology database. Retrieved from <http://www.ga.gov.au/geochron-sapub-web/geochronology/shrimp/search.htm>
- Page, R. W. (1996c). Sample 92-296 (Warramunga Formation). Geoscience Australia OZCHRON geochronology database. Retrieved from <http://www.ga.gov.au/geochron-sapub-web/geochronology/shrimp/search.htm>
- Page, R. W. (1996d). Sample 92-297 (Warramunga Formation). Geoscience Australia OZCHRON geochronology database. Retrieved from <http://www.ga.gov.au/geochron-sapub-web/geochronology/shrimp/search.htm>
- Page, R. W. (1996e). Sample 92-299 (Warramunga Formation). Geoscience Australia OZCHRON geochronology database. Retrieved from <http://www.ga.gov.au/geochron-sapub-web/geochronology/shrimp/search.htm>
- Page, R. W., Jackson, M. J., & Krassay, A. A. (2000). Constraining sequence stratigraphy in north Australian basins: SHRIMP U-Pb zircon geochronology between Mt Isa and McArthur river. *Australian Journal of Earth Sciences*, 47(3), 431–459. <https://doi.org/10.1046/j.1440-0952.2000.00797.x>
- Paton, C., Hellstrom, J., Paul, B., Woodhead, J., & Hergt, J. (2011). Iolite: Freeware for the visualisation and processing of mass spectrometric data. *Journal of Analytical Atomic Spectrometry*, 26(12), 2508–2518. <https://doi.org/10.1039/C1JA10172B>
- Pérez-Peña, J. V., Al-Awaddeh, M., Azañón, J. M., Galve, J. P., Booth-Rea, G., & Notti, D. (2017). SwathProfiler and NProfiler: Two new ArcGIS Add-ins for the automatic extraction of swath and normalized river profiles. *Computers & Geosciences*, 104, 135–150. <https://doi.org/10.1016/j.cageo.2016.08.008>
- Powell, J. W., Schneider, D. A., & Issler, D. R. (2018). Application of multi-kinetic apatite fission track and (U-Th)/He thermochronology to source rock thermal history: A case study from the Mackenzie Plain, NWT, Canada. *Basin Research*, 30, 497–512. <https://doi.org/10.1111/bre.12233>
- Quentin de Gromard, R., Kirkland, C. L., Howard, H. M., Wingate, M. T. D., Jourdan, F., McInnes, B. I. A., et al. (2019). When will it end? Long-lived intracontinental reactivation in central Australia. *Geoscience Frontiers*, 10(1), 149–164. <https://doi.org/10.1016/j.gsf.2018.09.003>
- Raimondo, T., Clark, C., Hand, M., Cliff, J., & Harris, C. (2012). High-resolution geochemical record of fluid–rock interaction in a mid-crustal shear zone: A comparative study of major element and oxygen isotope transport in garnet. *Journal of Metamorphic Geology*, 30(3), 255–280. <https://doi.org/10.1111/j.1525-1314.2011.00966.x>
- Raimondo, T., Clark, C., Hand, M., & Faure, K. (2011). Assessing the geochemical and tectonic impacts of fluid–rock interaction in mid-crustal shear zones: A case study from the intracontinental Alice Springs Orogen, central Australia. *Journal of Metamorphic Geology*, 29(8), 821–850. <https://doi.org/10.1111/j.1525-1314.2011.00944.x>
- Raimondo, T., Collins, A. S., Hand, M., Walker-Hallam, A., Smithies, R. H., Evins, P. M., & Howard, H. M. (2010). The anatomy of a deep intracontinental orogen. *Tectonics*, 29(4), TC4024. <https://doi.org/10.1029/2009tc002504>
- Raimondo, T., Hand, M., & Collins, W. J. (2014). Compressional intracontinental orogens: Ancient and modern perspectives. *Earth-Science Reviews*, 130, 128–153. <https://doi.org/10.1016/j.earscirev.2013.11.009>
- Ranalli, G. (2000). Rheology of the crust and its role in tectonic reactivation. *Journal of Geodynamics*, 30(1), 3–15. [https://doi.org/10.1016/S0264-3707\(99\)00024-1](https://doi.org/10.1016/S0264-3707(99)00024-1)
- Rawlings, D. J., Sweet, I. P., & Kruse, P. D. (2008). *Mount Drummond, Northern Territory: Explanatory notes* (SE 53-12, pp. 1–101). Northern Territory Geological Survey. Retrieved from <https://geoscience.nt.gov.au/gemis/ntgsjspui/handle/1/81809>
- Reno, B. L., Weisheit, A., Beyer, E. E., McGloin, M. V., & Kositsin, N. (2017). Proterozoic tectonothermal evolution of the northeastern sector of the Aileron Province. *Paper presented at the Annual Geoscience Exploration Seminar (AGES), Alice Springs, Northern Territory*. Retrieved from <https://geoscience.nt.gov.au/gemis/ntgsjspui/handle/1/85127>
- Reno, B. L., Weisheit, A., Beyer, E. E., Thompson, J. M., & Meffre, S. (2020). Summary of results. NTGS laser ablation ICP-MS in situ monazite petrochronology project: Constraining the chronologic history of the Delny and Entire Point shear zones, and the timing of metamorphism in the Aileron and Irindina provinces (NTGS Record 2020-008). Northern Territory Geological Survey. Retrieved from <https://geoscience.nt.gov.au/gemis/ntgsjspui/handle/1/90688>

- Roberts, J., & Engel, B. A. (1987). Depositional and tectonic history of the southern New England Orogen. *Australian Journal of Earth Sciences*, 34(1), 1–20. <https://doi.org/10.1080/08120098708729391>
- Rosenbaum, G. (2018). The Tasmanides: Phanerozoic tectonic evolution of eastern Australia. *Annual Review of Earth and Planetary Sciences*, 46(1), 291–325. <https://doi.org/10.1146/annurev-earth-082517-010146>
- Rosenbaum, G., Li, P., & Rubatto, D. (2012). The contorted New England Orogen (eastern Australia): New evidence from U-Pb geochronology of early Permian granitoids. *Tectonics*, 31(1), TC1006. <https://doi.org/10.1029/2011tc002960>
- Rudnick, R. L., McDonough, W. F., & O'Connell, R. J. (1998). Thermal structure, thickness and composition of continental lithosphere. *Chemical Geology*, 145(3), 395–411. [https://doi.org/10.1016/S0009-2541\(97\)00151-4](https://doi.org/10.1016/S0009-2541(97)00151-4)
- Sandiford, M., & Hand, M. (1998). Controls on the locus of intraplate deformation in central Australia. *Earth and Planetary Science Letters*, 162(1), 97–110. [https://doi.org/10.1016/S0012-821X\(98\)00159-9](https://doi.org/10.1016/S0012-821X(98)00159-9)
- Scrimgeour, I., & Raith, J. (2001). *Tectonic and thermal events in the northeastern Arunta Province* (Report 12, pp. 1–45). Northern Territory Geological Survey. Retrieved from <https://geoscience.nt.gov.au/gemis/ntgsjspui/handle/1/81548>
- Shaw, R. D., & Black, L. P. (1991). The history and tectonic implications of the Redbank Thrust Zone, central Australia, based on structural, metamorphic and Rb-Sr isotopic evidence. *Australian Journal of Earth Sciences*, 38(3), 307–332. <https://doi.org/10.1080/08120099108727975>
- Shaw, R. D., Langworthy, A. P., Offe, L. A., Stewart, A. J., Allen, A. R., & Senior, B. R. (1979). *Geological report on 1:100 000-scale mapping of the southeastern Arunta Block, Northern Territory* (Record 1979/47). A. Bureau of Mineral Resources.
- Skirrow, R. G., Cross, A. J., Lecomte, A., & Mercadier, J. (2019). A shear-hosted Au-Cu-Bi metallogenic event at ~1660 Ma in the Tennant Creek goldfield (northern Australia) defined by in-situ monazite U-Pb-Th dating. *Precambrian Research*, 332, 105402. <https://doi.org/10.1016/j.precamres.2019.105402>
- Spikings, R. A., Foster, D. A., & Kohn, B. P. (1997). Phanerozoic denudation history of the Mount Isa Inlier, northern Australia: Response of a Proterozoic mobile belt to intraplate tectonics. *International Geology Review*, 39(2), 107–124. <https://doi.org/10.1080/00206819709465262>
- Spikings, R. A., Foster, D. A., & Kohn, B. P. (2006). Low-temperature (<110°C) thermal history of the Mt Isa and Murphy Inliers, north-east Australia: Evidence from apatite fission track thermochronology. *Australian Journal of Earth Sciences*, 53(1), 151–165. <https://doi.org/10.1080/08120090500434609>
- Sueoka, S., Kohn, B. P., Tagami, T., Tsutsumi, H., Hasebe, N., Tamura, A., & Arai, S. (2012). Denudation history of the Kiso Range, central Japan, and its tectonic implications: Constraints from low-temperature thermochronology. *Island Arc*, 21(1), 32–52. <https://doi.org/10.1111/j.1440-1738.2011.00789.x>
- Tingate, P. R. (1990). *Apatite fission track studies from the Amadeus Basin, Central Australia* (PhD thesis), University of Melbourne.
- Traves, D. M. (1955). *The geology of the Ord-Victoria region, northern Australia* (p. 27). Bureau of Mineral Resources.
- Vermeesch, P. (2017). Statistics for LA-ICP-MS based fission track dating. *Chemical Geology*, 456, 19–27. <https://doi.org/10.1016/j.chemgeo.2017.03.002>
- Vermeesch, P. (2018). IsoplotR: A free and open toolbox for geochronology. *Geoscience Frontiers*, 9(5), 1479–1493. <https://doi.org/10.1016/j.gsf.2018.04.001>
- Wade, B. P., Hand, M., & Barovich, K. M. (2005). Nd isotopic and geochemical constraints on provenance of sedimentary rocks in the eastern Officer Basin, Australia: Implications for the duration of the intracratonic Petermann Orogeny. *Journal of the Geological Society*, 162(3), 513–530. <https://doi.org/10.1144/0016-764904-001>
- Wagner, G. A., & Van den haute, P. (1992). Fission-track dating. Kluwer Academic Publishers, Dordrecht.
- Walter, M. R., Elphinstone, R., & Heys, G. R. (1989). Proterozoic and Early Cambrian trace fossils from the Amadeus and Georgina Basins, central Australia. *Alcheringa: An Australasian Journal of Palaeontology*, 13(3), 209–256. <https://doi.org/10.1080/03115518908527821>
- Walter, M. R., Veevers, J. J., Calver, C. R., & Grey, K. (1995). Neoproterozoic stratigraphy of the Centralian Superbasin, Australia. *Precambrian Research*, 73(1), 173–195. [https://doi.org/10.1016/0301-9268\(94\)00077-5](https://doi.org/10.1016/0301-9268(94)00077-5)
- Weisheit, A. (2019). *Structural evolution of basement and basin rocks in the Jervois Range Special 1:100 000 mapsheet* (NTGS Record 2019-014). Northern Territory Geological Survey. Retrieved from <https://geoscience.nt.gov.au/gemis/ntgsjspui/handle/1/89782>
- Withnall, I. W., Golding, S. D., Rees, I. D., & Dobos, S. K. (1996). K–Ar dating of the Anakie metamorphic Group: Evidence for an extension of the Delamerian Orogeny into central Queensland. *Australian Journal of Earth Sciences*, 43(5), 567–572. <https://doi.org/10.1080/08120099608728277>
- Worden, K. E., Carson, C. J., Close, D. F., Donnellan, N. C., & Scrimgeour, I. R. (2008). *Summary of results. Joint NTGS-GA geochronology project: Tanami region, Arunta region, Pine Creek Orogen and Halls Creek Orogen correlatives, January 2005–March 2007* (NTGS Record 2008-003). Northern Territory Geological Survey. Retrieved from <https://geoscience.nt.gov.au/gemis/ntgsjspui/handle/1/82446>
- Yang, B., Collins, A. S., Blades, M. L., Munson, T. J., Payne, J. L., Glorie, S., & Farkaš, J. (2020). Tectonic controls on sedimentary provenance and basin geography of the Mesoproterozoic Wilton package, McArthur Basin, northern Australia. *Geological Magazine*, 159(2), 1–20. <https://doi.org/10.1017/S0016756820001223>
- Young, D. N., Edgoose, C. J., Blake, D. H., & Shaw, R. D. (1995). *Mount Doreen, Northern Territory: Explanatory notes* (pp. 1–55). Northern Territory Geological Survey. Retrieved from <https://geoscience.nt.gov.au/gemis/ntgsjspui/handle/1/81917>
- Zhan, Y., & Mory, A. J. (2013). Structural interpretation of the Northern Canning Basin, Western Australia. *Paper presented at the West Australian Basins Symposium, Perth, Western Australia*.

References From the Supporting Information

- Armstrong, J. T. (1988). Quantitative analysis of silicate and oxide minerals: Comparison of Monte Carlo, ZAF, and $\phi(\rho z)$ procedures. In D. E. Newbury (Ed.), *Microbeam analysis* (pp. 239–246). San Francisco Press.
- Chew, D. M., & Spikings, R. A. (2015). Geochronology and thermochronology using apatite: Time and temperature, lower crust to surface. *Elements*, 11(3), 189–194. <https://doi.org/10.2113/gselements.11.3.189>
- Donovan, J. J., Singer, J. W., & Armstrong, J. T. (2016). A new EPMA method for fast trace element analysis in simple matrices. *American Mineralogist*, 101(8), 1839–1853. <https://doi.org/10.2138/am-2016-5628>
- Donovan, J. J., & Tingle, T. N. (1996). An improved mean atomic number background correction for quantitative microanalysis. *Microscopy and Microanalysis*, 1, 1–7. <https://doi.org/10.1017/s1431927696210013>
- Doyle, N. (2010). *Fourth annual report for EL 24835, Phillip Creek, NT, period ended 15/8/2010* (CR2010-0505). Northern Territory Geological Survey. Retrieved from <https://geoscience.nt.gov.au/gemis/ntgsjspui/handle/1/75900>
- Drown, C. (2006). *Annual report for EL 7739 (Rover), 5 June 2005 to 4 June 2006* (CR2006-0224). Northern Territory Geological Survey. Retrieved from <https://geoscience.nt.gov.au/gemis/ntgsjspui/handle/1/85454>

- Flowers, R. M., Farley, K. A., & Ketcham, R. A. (2015). A reporting protocol for thermochronologic modeling illustrated with data from the Grand Canyon. *Earth and Planetary Science Letters*, 432, 425–435. <https://doi.org/10.1016/j.epsl.2015.09.053>
- Haines, P. W., & Scrimgeour, I. R. (2007). *Woodgreen, Northern Territory: Explanatory notes* (5753, pp. 1–28). Northern Territory Geological Survey. Retrieved from <https://geoscience.nt.gov.au/gemis/ntgsjspui/handle/1/81885>
- Ketcham, R. A., Carter, A., Donelick, R. A., Barbarand, J., & Hurford, A. J. (2007). Improved modeling of fission-track annealing in apatite. *American Mineralogist*, 92(5–6), 799–810. <https://doi.org/10.2138/am.2007.2281>
- Maidment, D. W. (2013a). Sample 2005080017 (Hill of Leaders Granite). Geoscience Australia OZCHRON geochronology database. Retrieved from <http://www.ga.gov.au/geochron-sapub-web/geochronology/shrimp/search.htm>
- Maidment, D. W. (2013c). Sample 2005080054 (Warramunga Formation). Geoscience Australia OZCHRON geochronology database. Retrieved from <http://www.ga.gov.au/geochron-sapub-web/geochronology/shrimp/search.htm>
- Mason, A. J. (1980a). *Final report – Exploration license 1427, Bowgan Creek NT* (CR1980-0118). Northern Territory Geological Survey. Retrieved from <https://geoscience.nt.gov.au/gemis/ntgsjspui/handle/1/70691>
- Mason, A. J. (1980b). *Final report – Field investigations EL 1235, Benmara NT* (CR1980-0143). Northern Territory Geological Survey. Retrieved from <https://geoscience.nt.gov.au/gemis/ntgsjspui/handle/1/60746>
- Page, R. W. (1996a). Sample 92-218 (Warrego Granite). Geoscience Australia OZCHRON geochronology database. Retrieved from <http://www.ga.gov.au/geochron-sapub-web/geochronology/shrimp/search.htm>
- Page, R. W., & Sweet, I. P. (1998). Geochronology of basin phases in the western Mt Isa Inlier, and correlation with the McArthur Basin. *Australian Journal of Earth Sciences*, 45(2), 219–232. <https://doi.org/10.1080/08120099808728383>
- Palmer, D. C. (1992). *Combined annual report for year ending 10th January, 1992* (CR1992-0183). Northern Territory Geological Survey. Retrieved from <https://geoscience.nt.gov.au/gemis/ntgsjspui/handle/1/61941>
- Smith, J. (2001). *Summary of results. Joint NTGS-AGSO age determination program 1999–2001* (NTGS Record 2001-007). Northern Territory Geological Survey. Retrieved from <https://geoscience.nt.gov.au/gemis/ntgsjspui/handle/1/82409>
- Southgate, P. N., Bradshaw, B. E., Domagala, J., Jackson, M. J., Idnurm, M., Krassay, A. A., et al. (2000). Chronostratigraphic basin framework for Palaeoproterozoic rocks (1730–1575 Ma) in northern Australia and implications for base-metal mineralisation. *Australian Journal of Earth Sciences*, 47(3), 461–483. <https://doi.org/10.1046/j.1440-0952.2000.00787.x>
- Ward, D. F. (1985). *EL 2835 – Helen Springs, Northern Territory, annual report for year ended 26th June 1985* (CR1985-0292). Northern Territory Geological Survey. Retrieved from <https://geoscience.nt.gov.au/gemis/ntgsjspui/handle/1/61320>